Article:

Ofune, M, Banks, P, Morina, A et al. (1 more author) (2016) Development of valve train rig for assessment of cam/follower tribochemistry. Tribology International, 93 (B). pp. 733-744. ISSN 0301-679X

https://doi.org/10.1016/j.triboint.2015.02.026

Development of Valve Train Rig for Assessment of Cam/Follower Tribochemistry

MacDonald Ofune, Paul Banks, Ardian Morina and Anne Neville
Institute of Functional Surfaces (IFS), University of Leeds, Leeds, LS2 9JT
E-mail: menmaof@leeds.ac.uk

ABSTRACT

Component bench tests are a crucial part of a tribology assessment experimental programme for most engines and subsystems. This is because they test the components under conditions simulating the operating characteristics of the system. These have become very important as they shed more light into the friction, wear, lubrication and importantly for this study, the tribochemistry of valve train systems. This work outlines the procedure for the development of a single cam rig (SCR) from a 1.25L FORD Zetec (SE) engine. Friction plots were used to validate the data obtained from the newly developed single cam rig with Mn-phosphate coated and polished follower against a cast iron camshaft. The tribofilm formed using normal and mid Sulphated Ash, Phosphorus and Sulphur (SAPS) 5W-30 oils were evaluated and correlated to the friction and wear properties of the tribopair.

Raman and FIB-SEM/EDX investigations of the tribochemical films showed that the normal SAPS oil produced patchy, thick (80-100 nm) and well dispersed tribofilm with better wear prevention capabilities. It was observed that Mid SAPS oil had lower wear prevention due to loosely dispersed and thin tribofilms. Absence of tribofilms at the centre of the insert with this oil also suggests that formation and removal processes are an integral part of the wear mechanisms in highly loaded cam follower systems.

1. Introduction

Environmental legislation calls for the use of engine lubricants with less impact on the environment in terms of exhaust emissions, while engine users demand more mileage per litre of fuel without any compromise on engine durability. From this standpoint, engine manufacturers require the optimum combination of materials, surface coatings and lubricant additive packages to minimize friction and wear in the piston, bearing and valve train components. The move from normal to mid and even ultra-low SAPS oils risks an increase in wear on engine tribocomponents. For this reason, there has been increased experimental work on the tribochemistry/tribology of 'low' SAPS containing oils against surface coatings, particularly DLC's and how they affect friction/wear of engine components-cam/follower tribopair.

Engine valve train friction contributions are typically from the valve guide/stem, camshaft bearings, bucket/tappet bore, and most importantly, cam follower interface, which accounts for approximately 80-90% friction contribution [1, 2]. Therefore, for improved engine efficiency, research into this tribopair is necessary. Accordingly, numerous authors have designed and used valve train rigs to study friction [3-7], wear [8-10], film thickness [11-14] and tribochemistry [15, 16] at the cam tappet contact. Historically speaking, Dyson and Naylor [3] were perhaps the first to investigate friction at the cam follower interface using a push rod assembly where the tappets were held in place by a pair of flat springs, and the corresponding stresses measured by means of piezo electric gauges.

Ito et al [8] studied the friction with the use of two strain gauges mounted on a push rod and shaft. Using both the deformation on the shaft and the force on the tappet, the friction coefficient was evaluated with a good degree of accuracy. The final apparatus was mounted on an engine for wear testing. A modern configuration of the cam/follower is the direct acting mechanical bucket type with a somewhat high sliding. Pieprzak et al [4] used the configuration to develop a valve train rig for the evaluation of friction due to tappet/bore rotation. This was achieved by preventing the tappet/bore assembly from rotating with a rigid mechanical quill. High tappet/bore frictions of 13% were recorded at low speed with lower values at high speed. In our study, this approach was not ideal as tribofilms are affected by tappet/bore motion and lubricant entrainment velocity.

A vast majority of the cam follower studies involve the use of a multiple cam rigs. In these types of rigs, camshafts have lobes at 90^0 from each other thus making computation of torque and relating it to a specific cam location more difficult. This is also coupled with system instabilities [17]. In order to understand different regions on the cam profile where significant friction and wear benefits can be achieved, it was pertinent to develop a single cam rig where the friction torque is investigated with respect to cam angle. Some aspect of this have been published in the literature [18, 19]. The rig is also furnished with high data recording and control with 1 data point for as low as 0.2^0 of camshaft rotation (1800 data points for one rotation of the camlobes). This will provide a better understanding of the cyclic processes in the cam follower contact and give us the ability to link the friction/wear properties to the tribochemical films across the camlobes and inserts.

Conducting tribochemistry studies of engine valve train systems is a very difficult task due to sliding/rolling motion, film thickness variation, and high loads/stresses experienced at the contact of interacting asperities. These dynamic variations cause a significant distinction on the tribofilm formation and removal across the cam profile and on the inserts. According to reports by Liu & Kouame [18], tribofilm investigations at seven locations on the cam profile ($\pm 14^o$, $\pm 10^o$, $\pm 4^o$ and cam nose-0^o degree) showed that the tribofilms were different at each location and were made up of short and long chain polyphosphate films in which temperature had a significant effect on their tenacity. Long chain polyphosphates tribofilms were shown to have good antiwear characteristics [18]. The formation/or reaction kinetics of polyphosphate film are strongly influenced by temperature. It has been reported that the bulk of the films are composed of short chain with long chain at the topmost surface but this structure can be altered in fully formulated oils [20, 21]. Similar findings with engine oil on metal surfaces have been reported to contain films composed of low concentrations of Zn, P, S with Ca and O as the topmost layer of the tribofilm [15]. These species have been reported to affect the antiwear properties of tribofilms [22, 23]. Uy et al [24] also investigated the tribofilms formed on tappets with Raman and observed Ca/Zn orthophosphate ($Zn_3(PO4)_2$), $CaCO_3$, Fe_3O_4 with some undecomposed hydrocarbon on the surface.

Currently, coatings/surface treatments are finding increased application in valve train systems. For instance, super finishing before deposition of TiN achieved 40% reduction in friction torque with 1-2% achievements in fuel consumption [5]. Similar results were obtained in a motored cam rig by super carburizing inserts to R_a of 0.09 μm [6]. The utmost in the use of coating architectures, is the sporadic increase in the use of DLC's in the improvement of cam follower friction/wear. DLCs have been touted for their low friction and wear-resistant properties in boundary/mixed lubrication. Friction coefficients as low as 0.006 have been reported in additivated oils [25]. However, due to vast DLC surface finishes available, these results are not general. DLC tribo properties are influenced by dopant elements, the quality of the oil, the submicron interlayers, and the need for adhesion of coating [26]. There is also a difference in their behaviour according to the interaction with oil additives which have conventionally been designed for ferrous surfaces [15, 27, 28].

It will be noteworthy to mention that the tribofilm removal rate, formation and stability are of utmost importance in highly loaded boundary/mixed tribological systems and so also in cam/followers. Gangopadhyay and coworkers [15] observed significant abrasive marks on DLC coated tappet in motored tests. This indicates a cyclic film removal process. There was also evidence in the tests performed on mixed sliding/rolling contacts by Haque et al.[17] on motored multiple valve train rig and MTM. SEM/XPS micrographs of the H-DLC coating revealed irregular polishing with the centre of the inserts showing high atomic species of the Cr interlayer while regions further from the centre revealed lower Cr in a ratio of 16.5:1. This indicates a high wear towards the centre of the inserts. Polishing can be very detrimental to engine components as the surfaces may lack the retention of engine lubricant necessary for the optimal operation. This heterogeneous polishing could be because the centre of the insert is in direct contact with the cam, flank, shoulder and ramp positions of the cam while further from the centre, contact is more predominant with the nose. Also, huge contact pressures lead to coating damage and peeling. Similar results have been reported by Kodai [29] on non-metal doped DLC coating deposited by RF plasma.

Furthermore, in commercial applications, DLC coatings have been tested in fired engine conditions to ascertain their performance in realistic operating conditions. In a recent paper by Durham and Kidson [10], fired engine tests were performed for 300 hrs on four different DLC coated tappets where they reduce camlobe wear by as much as 50-75 folds in the inlet/exhaust camshafts when compared with standard steel. However, it was observed that only one of the coatings tested (HHS) showed resistance to polishing, spallation and pitting wear. A similar approach has been employed on motored tests by Haque et al [17]. Using a different deposition process (unbalanced magnetron sputtering) from [10] in the production of W-DLC [29], no spallation or peeling was observed but the coating was worn from the surface in motorcycle stand tests.

Component bench rigs examine the tribopair under practice oriented engineering structures, thus better simulating the operating characteristics of the engine [30]. For instance, the friction characteristics of the inlet camlobe in a motored single cam rig, though, not identical with the conditions in an engine, have been reported to mirror those of the fired engine [31]. Consequently, bench /motored cam follower tribometers have become vital as they shed more light into the friction, wear, lubrication and more importantly, the tribochemistry of valve train systems.

This study outlines the development of a single cam follower rig for the study of tribochemistry on the inserts in boundary/mixed lubrication regime. It is the objective of this study to investigate the composition and thickness of the tribofilm and correlate this to friction and wear on the inserts. Mapping of tribofilm across the inserts has not been widely investigated. This study has shown that the thickness and composition of the tribofilm vary significantly, particularly at the centre of the insert. This is highly influenced by the oil type and temperature. Assessment of surface interactions with normal and mid SAPS oils on Mn-phosphate coated and polished inserts are discussed, as a means of validating the data obtained from the newly developed rig.

2. Rig Developmental Procedure

2.1. Modification of Engine Cylinder Head

Figure 1a shows a slice which was produced from a 1.25L Ford Fiesta Zetec (SE) engine with a double overhead camshaft (DOHC) and flat faced removable inserts in bucket arrangement. This was used in a non-fired mode and driven by a 2.2 kW ABB motor. The camshaft was slightly modified to accommodate the design configuration of the rig. This was achieved by sectioning the inlet camshaft into four bits in sets of 2 cam lobes each. At the ends of the new camshafts, holes were made to fasten them to stud shafts. The modified camshaft assembly is shown in Figure 1b. The clearance between the follower and base circle of the camlobes was maintained at 0.21-0.25 mm. This was achieved by using standard production inserts with slightly greater thickness from 2.60 to 2.70 mm. The centre of the camlobe was also slightly offset from the centre of the inserts to allow for some bucket/tappet rotation and reduce friction torque.

This shaft was then connected to high sensitivity torque transducer by means of flexible couplings to account for any misalignment. The plain bearings at the centre between the camlobes were grounded off to prevent any contact and eliminate friction at this point. The only bearing friction in the system came from two camshaft ball bearings.

2.2. Determination of Cam profile/Lift

In this engine, the inlet valve opens at 2^o before top dead centre (TDC) and 42^o after bottom dead centre BDC. This corresponds to camshaft duration of $112^o\left(\frac{180+42+2}{2}\right)$. The cam profile was determined with the aid of a digital dial indicator and protractor to an accuracy of $\pm1^o$. This was essential to understand the dynamic variations of forces on the system. A seven degree polynomial and cycloidal motion were obtained for the profile but the cycloidal motion produced the best fit. This motion is also better suited for high speed applications with less noise. The maximum lift was 9.80±0.20 mm (See Figure 2).

2.3. Calibration/Instrumentation

2.3.1 Cam Angle Triggering and Torque Measurement

A Hohner shaft encoder with a 720 pulse wheel was affixed at the end of the 20 mm modified camshaft by means of a non-conducting bellows. This was to ensure that there was no thermal drift on the shaft encoder and enable accurate cam angle triggering. The lag between channels enabled the torque monitoring while channel O represents a reference pulse. It has quadrature channels which could be split to give an angle encoding up to 0.125^o. The encoder index channel was used to synchronise the instantaneous torque reading (from the torque sensor) with the cam angle. Incremental pulses were used for torque monitoring at each rising edge.

2.3.2 Torque Transducer Speed and Torque Measurement

The speed and torque measurements were obtained from an RWT 421 torque transducer from Sensor Technology. It has a maximum torque rating of ±10 Nm. The shaft of the transducer measures the deflection once a torque is applied. The inbuilt surface acoustic wave evaluates the change in resonating frequency which is processed to give a torque/speed reading. It has an analogue dongle that enables rapid and large data capture when combined with the right NI-USB, hardware.

The torque transducer was calibrated from the manufacture at a ratio 1:1. On testing, no significant deviation from the value was observed, thus, no further calibration was required. Figure 3 show the typified linear relationship from the torque transducer calibration.

2.4. Materials

Tests were carried out using polished and standard production removable inserts of 16MnCr5 steel coated with soft running-in Mn-phosphate coating with thickness of 0.5-2.0 µm. SEM images of the polished inserts, Mn-phosphate inserts and chilled cast iron material are shown as Figure 4a, 4b and 4c respectively.

Figure 4d shows removable inserts that are force fitted onto the buckets in the SCR assembly. Once the rig was heated up, they expand and remain tightly in place. Mn-phosphate and polished inserts had Ra of 0.25 µm and 0.035 µm respectively. The camshaft is chromium chilled cast iron with R_a 0.055 µm. Lubricants used for the tests are two European SAE 5W30 fully formulated mid and normal SAPS oil from TOTAL, hereafter referred to as oil A and oil B respectively. Table 1 give details of the concentration of key elements in the engine oils.

Before changing the lubricant to be used on the SCR, the former lubricant was drained off, and the rig was first flushed with base oil at high pressure of 7 psi (20 L/m) for 2 hrs. This was to remove any residual oil within the hoses and cylinder head. The rig was then disassembled, and cleaned with iso-propanol and high detergency fluid. It was left to dry for 24 hrs before the bath was loaded with the next fresh oil.

2.5. Valve Train Friction Torque

The data collected from the analogue end of the torque transducer were passed into an NI-USB 6212 hardware giving characteristic waveforms that give information about the speed of the camshaft assembly. The natural frequency within the test bench was about 400 Hz and filtering with a Butterworth filter to the 6^{th} degree at a frequency of 395-405 Hz did not affect the friction torque. Deviations were in the range of ±5 mNm Similar findings have been reported by Mufti [32]. Essentially, the instantaneous torque is made up of friction and geometric components. During valve openings, energy is absorbed by the spring and this is released to the camshaft as torque. The friction component is very high during valve opening and has little or no components during valve closing. The inertia/geometric torque on the other hand have equal positive and negative components during valve opening and closing. Ideally, by taking mean torque values over the cam cycle, the inertia/geometric torque will be effectively cancelled out leaving the friction component [4, 31, 33]. The average friction torque was obtained by taking an average of the 200 data points obtained for each camshaft cycle. This corresponds to approximately 1 data point for every 1.8^o of cam shaft rotation. This was then averaged over the duration of the test in the steady state region.

Due to the compact and rigid nature of the modified camshaft and entire single cam rig assembly, the system was able to operate at high speed (up to 3000 rpm) with limited noise. Figure 5a and 5b shows the output torque values shown at 300 and 2100 rpm respectively. At 2100 rpm, the entire torque curve (35 cycles) was not shown because the image will be crammed together. Only the first 5 cycles were shown to demonstrate the low vibration of the rig at high speed. The asymmetric nature of the torque curve is due to work done by the camshaft during valve opening. This constitutes both geometric and the bulk of friction torque. On valve closing, work is done by the valve spring in maintaining contact with the camshaft which essentially consists of all geometric components. At high speed, the work done by the camshaft is slightly greater than those of the spring. This difference is proportional to the friction torque which is typically low at high camshaft speeds.

2.6. Test Procedure

The lubricant bath consists of a 5L reservoir which was filled with the set amount of lubricant for the test. The system was raised to the required test temperature by the oil bath. Two test temperatures of 75^0C and 105^0C were used for the validation testing on the newly developed rig. The oil was maintained at the test temperature by HAAKE DC200 oil bath with a sensitivity of $\pm 0.10^0$C. LabView software was used to plot the temperature rise which typically took 3-5 minutes for the lubricant to reach the set temperature but this was pumped through the rig to heat up the entire setup, which generally took 30 mins. The lubricant supply to the camlobe and follower well was controlled by check valves in contact with a 6 mm hose. Figure 6a shows the entire schematic of the single cam rig setup. The flow rate was maintained at 7.5-8.0 g/minute with a pressure of 6.0 psi. The maximum load applied to the cam by the spring loaded valve/collet assembly was 1286 N which resulted in a mean contact pressure of 0.75 GPa. The valve train friction torque was measured with the aid of a torque transducer which was in-line with the camshaft and motor spindle. This data was collected from the analogue section of the torque transducers at minimum of 1 data point for every 1.8^0 of camshaft rotation in 7.5 minutes intervals. This was achieved with DAQ 6212 hardware with a capacity of 400 K Samples/seconds. Further processing to obtain the average friction torque at specified interval was also achieved with LabView and this was transferred to the PC system. The schematic diagram of the single cam follower test rig is shown in Figure 6a. The average friction torque was recorded at camshaft speeds of 300, 600, 1000, 1200, 1500, 1800 and 2100 rpm but all data captured during ramping conditions were discarded due to fluctuations in torque values. Elimination of torque data at the instance of speed increase has also been used by Durham and Kidson [10]. This enabled the monitoring of the friction torque value until a steady state value was obtained, for about 45 minutes. Only then was the speed increased to the next level. The test profile for the test can be divided into two section of the running-in phase and the steady state phase as shown in Figure 6b. Similar procedures have been used by Gangopadhyay [34] and Broda [26]. Numerical calculations using the Dowson and Higginson equation for line contact at the cam follower interface revealed that the oil film thickness lies between 0.06-0.20 µm, based on the speed range used in the study. The composite surface roughness was 0.25 µm and 0.065 µm for the Mn-phosphate and polished insert respectively. This gave a specific film thickness (λ ratio) between 0.24-3.70 µm (mixed regime).

Only one pair of camshaft and bucket was used during the test. After each test, the camshafts were cleaned with acetone to remove any tribofilm on the surface. This was to ensure that the film will not affect the next result. This camshaft has also been used for past testing in the development of the rig. The used tappet/bucket had R_a value of 0.025 µm. Both camshaft and bucket were considered broken-in. Only the inserts were changed for each set of tests. The breaking-in period was typically between 4-5 hrs because the surfaces had similar R_a with those used in [34] . The test procedure had three basic objectives;

1) Observe if the newly developed rig had good sensitivity for differentiating the friction

properties of two different oils and coatings.
2) Check for repeatability of the data produced from the new bench test apparatus.
3) Investigate the tribofilms formed on the inserts.

2.7. Raman Surface Test Procedure

Raman spectroscopy is a very useful technique for the determination of the structure of the tribofilm which have been formed on the surface. Raman technique has a probing depth in excess of the thickness of the tribofilm, hence it will probe the substrate structure as well as those of the tribofilm. The change in counts due to increase in accumulation can be attributed to the re-ordering of the molecule while Raman shift indicates stretching of the molecules. The samples were exposed for 10secs at 488nm wavelength with laser power of 100 % at 2 accumulations. Higher accumulations help reveal narrow adsorption bands of molecules which may not have been seen at lower accumulations. Small spot sizes of 20 µm x 20 µm were chosen as the sampling region. Numerous spectra were obtained in this region to ensure the results were repeatable. Spectra of wear scar were taken at three selected points approximately 0.5 mm from centre (P1), on the edge of concentric circles (P2) and at the edge of the inserts (P3), to identify the tribochemical films which were formed on the surface. These are further discussed in section 3.5.2 of this report. Based on the conditions used, the laser power reaching the surface was only a few milliwatts to prevent surface damage.

2.8. FIB – SEM Imaging Procedure

The FIB-SEM technique was used to observe the tribofilm on the surface before future TEM surface analytical tests were carried out. Platinum deposition of 10.00 µm x 2.00 µm x1.00 µm volumes was carried out at 0.3 nA. Bulk removal with an ion source of Gallium was carried out at 7 nA to create a volume of 10.00 µm x 6.00 µm x3.00 µm. Then a cleaning cross section was done at 1nA. Further cleaning cross sections were carried out at 0.3 nA with volume of 10.00 µm x 0.5 µm x1.50 µm to remove the curtaining effect and produce FIB-SEM images.

3. Results and Discussion

3.1. Friction Data

Figure 7a and 7b show the good repeatability of the data obtained from the newly developed valve train rig with a standard cast iron camshaft against polished production inserts and Mn-phosphate inserts respectively. The difference in friction torque is a small fraction of the final insert finish observed between each sample. The variability observed at low temperature is slightly greater for all the speed range tested. Oil A was used for the test at an oil supply temperature of 105^0C. All tests were performed three times and the average friction torque from all tests was used as the basis for comparison with other experimental conditions. The average friction torque reduces with increasing speed due to lubricant entrainment velocity into the cam follower contact region. The reduction profile also depicts the mixed lubrication regime of the Stribeck diagram which moves from a more boundary dominated regime at low speed to more elastohydrodynamic regimes at high speeds. An increase in friction torque is also observed with increasing temperature (Figure 7c) and this has been reported in previous studies [32, 35].

3.2. Effect of Surface Finish on Average Friction Torque

The effects of surface finish on the average friction torque are displayed in Figure 8 (a) and (b). Friction torque benefits were achieved by the polished insert at higher temperature of 105^0C for all speeds tested. At low temperature of 75^0C, the frictional responses between these surfaces are marginally different for most speeds tested. This is particularly due to the viscosity of the lubricant which forms thick films between the interacting surfaces. At 105^0C and 300 rpm, however, the polished insert and Mn-phosphate coating have specific film thickness (λ) 0.95 and 0.24 respectively. At this speed, greater friction benefits are achieved due to boundary lubrication where formation of molecular tribofilms controls the frictional responses of the system. The effect of surface roughness is also an important factor for the improvement of friction because it controls the asperity contact which affects both friction and wear in boundary lubrication. Similar friction benefits have been observed when polished inserts were compared with Mn-phosphate coating [36]. Although, Mn-phosphate is widely used in cam/follower inserts and piston liners as soft running–in coatings [36, 37] and for adhesive wear prevention because the coating has a crystalline, porous, soft and rougher surface finish (See Figure 4) which gives good oil wettability, absorbance and oil retention characteristics [38]. The high friction of the coating can be attributed to high asperity interaction between the insert and cam surface coupled with less reactivity with lubricant additives, which were conventionally designed for ferrous surfaces. For the speed range tested (300-2100 rpm), the Mn-phosphate coating had a specific film thickness (λ) in the range from 0.24 -1.00. This are considerably lower than the polished insert which have a λ ratio from 0.95 – 3.7 for the speed range tested. It thus suggests that the polished insert is predominantly in the mixed regime. SEM micrograph discussed in section 3.5.1 also suggests that the $Mn_3(PO_4)_2$ surfaces are less resistant to abrasive wear.

3.3. Effects of Engine Oil Formulation

Oil formulations have a crucial part to play in the reduction of friction and wear in boundary/mixed lubricated contacts. Previous studies [34] have shown that fully formulated oil with 700 ppm of MoDTC reduced the friction torque by 29% and the friction torque were independent of camshaft speed/surface coatings. This was attributed to the formation of MoS_2 sheets which have weak Van der Waals interactions between layers and covalent bond between atomic species [34, 39]. These tribolayers control friction on interacting surface [34]. In our application, oil A was an ester based friction modified fully formulated oil and the friction benefits (Figure 9a) can be observed across the entire speed range although significant benefits are experienced at low speed. Improvements at high speed are due to the differences in the bulk properties of both lubricants particularly their viscosity [40]. Oil A was observed to reduce the friction in polished inserts by approximately 29 %.

Ideally, the resultant of the forces on the follower, the inertia and spring forces should remain unchanged with the introduction of a new type of lubricant. Lower torque responses can therefore be attributed to the ability of the lubricant to reduce friction torque. Evaluation of the instantaneous torque across the cam profile revealed that significant friction torque benefits were achieved with oil A at all regions with maximum improvements at approximately -73^o from the cam nose. This is the region of high loads and similar findings have been reported in [31] . The results were computed for the camshaft speed of 300 rpm in predominantly boundary lubrication (See Figure 9b). The rising part of the cam showed more benefits as this is the region in which significant work is done by the camlobes. From Figure 9b, oil A will result in a maximum of 14% reduction in power consumption at 300 rpm.

3.4. Insert Wear Measurement

At the end of the test, the wear on the insert was traced by an NPFLEX White Light Interferometry as shown in Figure 10. Significant wear regions were characterized by the presence of ridges on the inserts. At the edge of the insert, contact with the cam lobe occurs but this does not produce significant grooves or valley on the surface of the inserts. At the centre, however, there are contacts with the cam nose, flank, shoulder and ramp regions, and as such, the wear depth (WD) was greatest in this region. The insert surface showed concentric circles with different width. Similar findings have been reported by [14]. This can be attributed to edge loading effects and tappet rotation within the tappet bore which allows circumferential rubbing action to take place on the inserts with dimensions greater than the camlobe width. The sum of the wear depth at the insert centre and the wear scar width was used to determine the maximum wear depth. These approaches have been employed by Kano [19] and Liu [18] for the evaluation of wear on camlobes.

3.4.1 Effects of Oil Type on Wear

Oil B was observed to reduce the wear for most of the conditions and material pairs tested. The surfaces of the inserts with oil B show a very distinct distribution of dark antiwear films on the surface which have good extreme pressure properties necessary to reduce wear. For the $Mn_3(PO_4)_2$ the high wear could be due to the high temperature ploughing of the soft running-in Mn-phosphate coating during tribological tests (see figure 11a & 11b). With oil A, high temperature affected both distribution and durability of the tribofilm. This was not observed with oil B which was composed of a primary ZDDP. On polished inserts, oil B produced a marginal difference in wear.

In fully formulated engine lubricants, synergistic, antagonistic and harmless interactions are all possible. In a recent paper by Fujita et al. [41], it was observed that antiwear films undergo antagonistic interactions in the presence of dispersant and load, with secondary ZDDP being more susceptible to attack. Film thicknesses could be as high as 80 – 120 nm in ZDDP additivated oils but could reduce to less than 20 nm in the presence of dispersant and load [41]. There have even been reports where no films were observed [42] due to antagonistic interactions with dispersants.

3.5. Surface Analytical/Tribochemistry Studies

3.5.1 Scanning Electron Microscopy/Energy Dispersive X-rays (SEM/EDX)

The significant difference between the surfaces of the inserts has to do with the polishing and abrasive wear of the inserts as well as the distribution of the tribofilm on the surface. The polished shim in Figure 12a showed a heterogeneous distribution of the lubricant derived films with little/no scoring marks on the surface. White patches were identified as Ca concentrated areas, particularly $CaCO_3$ derived from the detergent/dispersant used in the oil with a matrix of phosphorus embedded underneath. This is shown at regions 5 & 6. The presence of $CaCO_3$ and phosphate has been supported by Raman analyses which are discussed in the next section. At higher temperature (Figure 12b), significant abrasive marks were observed on the worn surface with patchy phosphate films which appear to have been slightly removed due to rubbing action from the camlobe. These abrasive processes cause lots of third body wear particles due to plastic deformation and large nascent surfaces that can be quickly oxidised. In extreme cases, this can lead to catastrophic failures. EDX information revealed phosphorus concentrations (atomic %) of 0.70 % at regions 1, 2 and 3 respectively. At region 4 on the wear scar, the phosphorus concentration was 0.08 %. Zn concentration typically ranged from 0-0.24 % at regions 1-3, to 0.18 % at region 4. It is worthwhile to mention that at most regions of the wear track investigated, the Zn concentration was very low and even absent in some areas as shown in Table 2. This region was at the centre of the insert. This clearly illustrates the heterogeneous nature of lubricant derived tribofilms as well as the inherent surface sensitivity of this technique. Examination of the Mn-phosphate inserts showed parallel/horizontal scoring marks at both temperatures (Figure 12c & 12d). At lower temperature, however, this resulted in a smoother surface while at high temperature, the surface were rougher consisting of ridges/grooves on the surface of the insert.

The low levels of Zn, P, and S of the tribofilm on the wear track at points 1,2, 3, and 4 clearly reduces the antiwear properties on the inserts [23]. This could be as a result of the dispersant used in the oil. Certain dispersant particularly polyisobutyl succinimide polyamine (PIBSA PAM) have been reported to suppress the formation of antiwear films [42]. The absence of S on all regions examined on the insert at 105^0C is still unclear. In addition, the high phosphorus concentration formed on the inserts at 75^0C supports their good antiwear characteristics. These results suggests that the durability of antiwear films are strongly affected by temperature even though high temperature have been reported to favour the formation of thick padlike antiwear phosphate films [43, 44]. In addition, the efficacy of the tribofilm is influenced by the equilibrium between film removal, formation and associated mechanical properties [45].
Recent studies on camlobes [18] with secondary ZDDP have shown that high temperature affect the durability of these films, which supports the finding in this work. It will be worthwhile to investigate the mechanical and rheological properties of these films but this is beyond the scope of the present study.

Oil A produces tribofilms that are thin and sparsely distributed on the surface as shown in Figure 12b. These suggest that during rubbing, direct asperity interactions are more likely to occur, thus increasing the likelihood of insert wear. Using oil B, Figure 12e and 12f show the SEM image of the tribofilm formed on the surface of the polished insert. Continuous padlike layers that are separated by craters were observed on the insert surface although this was more conspicuous at 105^0C. This has been reported for model oils containing ZDDP [46]. The films appear significantly thicker and more evenly distributed on the surface than oil A. This minimizes the asperity contact and clearly helps improve wear on the inserts.

3.5.2 Raman Spectroscopy – Investigation of Film Structure

Figure 13 shows methodology which was used to map the tribofilm on the inserts. The Raman image of the wear scar region analyzed with the selected spot size as shown in Figure 13a 13b and 13c. Similar points were used for the FIB-SEM images. Figure 14a & b showed the Raman spectra of the films formed on the wear track of the polished inserts at 105^0C using oil A and oil B. Raman spectra of an unused sample was shown as P for comparison. The tribofilm from both oils have similar characteristics or film structures at P2 and P3. The narrow shoulders at 964-975 cm^{-1} are fingerprints of zinc/calcium orthophosphate [47]. These are obvious at 105^0C than 75^0C, suggesting thicker films at higher temperature (Raman spectra's at 75^0C are not shown). Other components of the tribofilm within the wear scar are FeS_2 with peaks at 330-341 cm^{-1}. Narrow bands at 527-530cm^{-1} may be internal vibrations of PO_4^{3-} [48] or an iron oxide [47]. The peaks at 901-920 cm^{-1} are due to bending of the phosphate from the secondary antiwear additive. At 1040-1105 cm^{-1}, calcium carbonate peaks were observed from the detergent used in the oil. Spectra of oil A at P1 showed some fingerprints Fe_3O_4 at 675-680 cm^{-1} which was not observed at other points. Minor peaks of phosphates and carbon were also seen on the contact region at 960 cm^{-1} and 1350/1550 cm^{-1} respectively. Peaks at 2736-2748 cm^{-1} are due to undecomposed hydrocarbon on the insert surface.

At the centre of the inserts (P1), oil B produced tribofilms which had similar spectras with points P2 and P3. Oil A had a different spectrum at the centre of the insert at 105^0C. The films compose of Fe_3O_4 and FeS_2 with no indication of phosphate films. These have been supported by FIB-SEM images in section 3.5.2. This suggests that the tribofilms derived from oil A are easily removed at the center of the insert due to rubbing action from the camlobes in highly loaded non-conformal valve train contacts.

3.5.3 FIB-SEM Results

Oil A produced a very thin film (ca.2-5 nm) at the centre of the inserts while ca. 54-68 nm thick tribofilm was formed at P2. This huge discrepancy can be attributed to the removal action due to high pressure rubbing action (from the ramp, flank, shoulder and nose) of the camlobe at the centre of the insert. The presence of subsurface cracks at the centre of the insert was also observed which indicates that the deformation process extends beyond the thin nanoscopic films into the base of the material and suggests that the tribofilm has low tenacity. This also indicates that the film thicknesses influences the wear as this has been reported by Zhang et al [42]. At other points, no cracks were seen since the films formed reduced and modified the wear processes. At P2, intermittent rubbing occurs due to edge loading and rotation of the tappet in the tappet bore. Oil B forms significant tribofilms at both the centre of the inserts (P1) and at P2 (See Figure 15). The thickness of the tribofilm formed by oil B is considerably higher than those observed with oil A. At the centre, oil B formed tribofilms about ca. 80-86 nm thick which was about 16-40 times thicker than oil A. This clearly supports the initial Raman investigation of the presence of the tribofilm at the centre of the inserts. At P2 however, oil B formed films ca. 100nm thick while oil A produced tribofilms ca. 68 nm thick. Going through the wear depth on the inserts and SEM micrographs, the development of stable, uniform and well dispersed tribofilms is an essential requirement for low wear rates. Difference in thickness of these tribofilms at P1 and P2 supports a removal and formation process. This may be due to load/pressure variations, flash temperatures and reactivity/or interaction with the oil on the substrate.

4. Conclusions

Tribological tests and post mortem surface analytical tests of Raman, and FIB-SEM/EDX have been used to investigate the structure, film thickness and composition of the tribofilms formed by both oils with the coating architectures of Mn-phosphate, and polished inserts The use of these multiple techniques helps shed more light on the composition of the tribofilms on the surface of inserts and enables us to establish correlation with the wear mechanisms. The findings of this work can be summarised as follows;

- A single cam rig has been developed, that has high sensitivity to distinguish the frictional responses of surface coatings as well as fully formulated lubricants with very close chemistries.

- Good repeatability and consistency from the experimental protocol for the validation tests indicates that the newly developed rig, its instrumentation, data processing/acquisition and operational procedures are reliable. They can provide valid information with confidence. For instance the increase of friction torque with increasing temperature has been widely reported by other researchers.
- Tribochemical investigations of the inserts are also in close agreement with previous studies. Temperature and additive concentration appear to affect the distribution of phosphate films on the inserts. More densely packed films were observed at 105^0C on inserts tested with oil B which has a higher concentration of primary ZDDP additives. This resulted in better wear prevention.
- The composition and structure of the tribofilm has a huge impact on the friction and wear response of the system. The presence of Zn, P, and S were shown to have significant impact of the antiwear properties of the tribofilm. They have been shown to affect the durability of the films on the surface. Further surface analytical tests will shed more light on the interatomic layered tribofilm derived by both oils.

5. Acknowledgements

This study was funded by the FP7 program through the Marie Curie Initial Training Network (MC-ITN) entitled “ENTICE - Engineering Tribochemistry and Interfaces with a Focus on the Internal Combustion Engine” [290077] and was carried out at University of Leeds.

6. References

[1] M. Kano, "Super low friction of DLC applied to engine cam follower lubricated with ester-containing oil," Tribology International, vol. 39, pp. 1682-1685, 2006.

[2] Comfort, Allen. An introduction to heavy-duty diesel engine frictional losses and lubricant properties affecting fuel economy-Part I. No. 2003-01-3225. SAE Technical Paper, 2003.

[3] A. Dyson and H. Naylor, "Application of the Flash Temperature Concept to Cam and Tappet Wear Problems," Proceedings of the Institution of Mechanical Engineers: Automobile Division, vol. 14, pp. 255-280, January 1, 1960 1960.

[4] Pieprzak, J. M., P. A. Willermet, and D. P. Dailey. Experimental evaluation of tappet/bore and cam/tappet friction for a direct acting bucket tappet valvetrain. No. 902086. SAE Technical Paper, 1990.

[5] Masuda, Michihiko, Masato Ujino, Kenji Shimoda, Kouji Nishida, Ikuo Marumoto, and Yuhji Moriyama. Development of titanium nitride coated shim for a direct acting OHC engine. No. 970002. SAE Technical Paper, 1997.

[6] Ahn, Seung Gyun, Hyung Oh Ban, Bong Lae Jo, Seung Cheal Kim, and Seung Cheal Jung. Development of supercarburized tappet shim to improve fuel economy. No. 2000-01-0613. SAE Technical Paper, 2000.

[7] Kanzaki, Tatsuo, Nobuo Hara, Akiyoshi Mori, and Kizuku Ohtsubo. Advantage of Lightweight Valve Train Component on Engines. No. 980573. SAE Technical Paper, 1998.

[8] Ito, Akemi, Lisheng Yang, and Hideo Negishi. A Study on Cam Wear Mechanism with a Newly Developed Friction Measurement Apparatus. No. 982663. SAE Technical Paper, 1998.

[9] J. E. Booth, T. J. Harvey, R. J. K. Wood, and H. E. G. Powrie, "Scuffing detection of TU3 cam–follower contacts by electrostatic charge condition monitoring," Tribology

International, vol. 43, pp. 113-128, 2010.
[10] J. Durham and A. Kidson, "The effects of low sulfated ash, phosphorus and sulfur oils on camshaft/tappet tribocouples with various diamond‐like‐carbon coated tappets in motored and fired engines," Lubrication Science, 2014.
[11] G. M. Hamilton, "The hydrodynamics of a cam follower," Tribology International, vol. 13, pp. 113-119, 1980.
[12] D. Dowson, P. Harrison, C. Taylor, and G. Zhu, "Experimental observation of lubricant film state between a cam and bucket follower using the electrical resistivity technique," in Proceedings of the Japan international tribology conference, 1990, pp. 119-124.
[13] M. Soejima, Y.Ejima, Y.Wakuri, and T.Kitahara, "Improvement of Lubrication for Cam and Follower," Tribology Transactions, vol. 42, pp. 755 - 762, 2008.
[14] G. Zhu, "A Theoretical and Experimental Study of the Tribology of a Cam and Follower," Doctor of Philosophy, Mechanical Engineering PhD Thesis, University of Leeds 1988.
[15] A. Gangopadhyay, K. Sinha, D. Uy, D. G. McWatt, R. J. Zdrodowski, and S. J. Simko, "Friction, Wear, and Surface Film Formation Characteristics of Diamond-Like Carbon Thin Coating in Valvetrain Application," Tribology Transactions, vol. 54, pp. 104-114, 2010/12/01 2010.
[16] A. K. Gangopadhyay, R. O. Carter, S. Simko, H. Gao, K. K. Bjornen, and E. D. Black, "Valvetrain Friction and Wear Performance with Fresh and Used Low-Phosphorous Engine Oils," Tribology Transactions, vol. 50, pp. 350-360, 2007/06/26 2007.
[17] T. Haque, A. Morina, and A. Neville, "Tribological performance evaluation of a hydrogenated diamond-like carbon coating in sliding/rolling contact–effect of lubricant additives," Proceedings of the Institution of Mechanical Engineers, Part J: Journal of Engineering Tribology, vol. 225, pp. 393-405, 2011.
[18] E. Liu and S. D. Kouame, "An XPS Study on the Composition of Zinc Dialkyl Dithiophosphate Tribofilms and Their Effect on Camshaft Lobe Wear," Tribology Transactions, vol. 57, pp. 18-27, 2014/01/02 2013.
[19] M. Kano and I. Tanimoto, "Wear mechanism of high wear-resistant materials for automotive valve trains," Wear, vol. 151, pp. 229-243, 1991.
[20] M. L. S. Fuller, M. Kasrai, G. M. Bancroft, K. Fyfe, and K. H. Tan, "Solution decomposition of zinc dialkyl dithiophosphate and its effect on antiwear and thermal film formation studied by X-ray absorption spectroscopy," Tribology International, vol. 31, pp. 627-644, 1998.
[21] J. M. Martin, C. Grossiord, T. Le Mogne, S. Bec, and A. Tonck, "The two-layer structure of Zndtp tribofilms: Part I: AES, XPS and XANES analyses," Tribology International, vol. 34, pp. 523-530, 2001.
[22] H. Spikes, "Low‐ and zero‐sulphated ash, phosphorus and sulphur anti‐wear additives for engine oils," Lubrication Science, vol. 20, pp. 103-136, 2008.
[23] S.-H. Choa, K. C. Ludema, G. E. Potter, B. M. DeKoven, T. A. Morgan, and K. K. Kar, "A model for the boundary film formation and tribological behavior of a phosphazene lubricant on steel," Tribology Transactions, vol. 38, pp. 757-768, 1995.
[24] Uy, Dairene, Steven J. Simko, Ann E. O'Neill, Ronald K. Jensen, Arup K. Gangopadhyay, and Roscoe O. Carter. Raman characterization of anti-wear films formed from fresh and aged engine oils. No. 2006-01-1099. SAE Technical Paper, 2006.
[25] M. Kano, Y. Yasuda, Y. Okamoto, Y. Mabuchi, T. Hamada, T. Ueno, J. Ye, S. Konishi, S. Takeshima, and J. Martin, "Ultralow friction of DLC in presence of glycerol mono-

oleate (GNO)," Tribology Letters, vol. 18, pp. 245-251, 2005.
[26] M. Broda and R. Bethke, "Friction Behavior of Different DLC Coatings by using Various Kinds of Oil," SAE Int. J. Mater. Manuf., vol. 1, pp. 832-840, 2008.
[27] S. Equey, S. Roos, U. Mueller, R. Hauert, N. D. Spencer, and R. Crockett, "Tribofilm formation from ZnDTP on diamond-like carbon," Wear, vol. 264, pp. 316-321, 2008.
[28] T. Haque, A. Morina, A. Neville, R. Kapadia, and S. Arrowsmith, "Effect of oil additives on the durability of hydrogenated DLC coating under boundary lubrication conditions," Wear, vol. 266, pp. 147-157, 2009.
[29] Kodai, A., T. Mori, and T. Inukai. Applying hard thin coatings to tappets to reduce friction. No. 2001-01-1886. SAE Technical Paper, 2001.
[30] J. R. Davis, "Friction and Wear of Internal Combustion Engine Parts," ASM Handbook, vol. 18, pp. 553 - 560, 1992.
[31] R. Mufti and M. Priest, "Effect of cylinder pressure on engine valve-train friction under motored and fired conditions," Proceedings of the Institution of Mechanical Engineers, Part J: Journal of Engineering Tribology, vol. 226, pp. 306-314, April 1, 2012 2012.
[32] R. A. Mufti and M. Priest, "Experimental and theoretical study of instantaneous engine valve train friction," Transactions of the ASME. Journal of Tribology, vol. 125, pp. 628-37, 07/ 2003.
[33] P. A. Willermet, J. M. Pieprzak, and D. P. Dailey, "Tappet Rotation and Friction Reduction in a Center Pivot Rocker Arm Contact," Journal of Tribology, vol. 112, pp. 655-661, 1990.
[34] A. Gangopadhyay, E. Soltis, and M. Johnson, "Valvetrain friction and wear: influence of surface engineering and lubricants," Proceedings of the Institution of Mechanical Engineers, Part J: Journal of Engineering Tribology, vol. 218, pp. 147-156, 2004.
[35] D. Zhu and H. S. Cheng, "Vehicle Tribology - Tribological Performance Ceramic Roller Followers/Camshaft System in Automobile Valve Trains," Tribology Series 18, vol. 18, pp. 149 - 156, 1991.
[36] A. Gangopadhyay, D. G. McWatt, R. J. Zdrodowski, S. J. Simko, S. Matera, K. Sheffer, and R. S. Furby, "Valvetrain Friction Reduction through Thin Film Coatings and Polishing," Tribology Transactions, vol. 55, pp. 99-108, 2012/01/01 2011.
[37] T. S. Eyre and B. Crawley, "Camshaft and cam follower materials," Tribology International, vol. 13, pp. 147-152, 1980.
[38] B. J. Taylor and T. S. Eyre, "A review of piston ring and cylinder liner materials," Tribology International, vol. 12, pp. 79-89, 1979.
[39] A. Morina, A. Neville, M. Priest, and J. H. Green, "ZDDP and MoDTC interactions in boundary lubrication-The effect of temperature and ZDDP/MoDTC ratio," Tribology International, vol. 39, pp. 1545-1557, 2006.
[40] M. Priest, "Introduction to Tribology," vol. 1, pp. 1 -76, 2011.
[41] H. Fujita, R. P. Glovnea, and H. A. Spikes, "Study of Zinc Dialkydithiophosphate Antiwear Film Formation and Removal Processes, Part I: Experimental," Tribology Transactions, vol. 48, pp. 558-566, 2005/10/01 2005.
[42] J. Zhang, E. Yamaguchi, and H. Spikes, "The Antagonism between Succinimide Dispersants and a Secondary Zinc Dialkyl Dithiophosphate," Tribology Transactions, vol. 57, pp. 57-65, 2014/01/02 2013.
[43] H. Fujita and H. A. Spikes, "Study of Zinc Dialkyldithiophosphate Antiwear Film Formation and Removal Processes, Part II: Kinetic Model," Tribology Transactions, vol. 48, pp. 567-575, 2005/10/01 2005.
[44] H. Spikes, "The history and mechanisms of ZDDP," Tribology Letters, vol. 17, pp. 469-89, 2004.

[45] S. Bec, A. Tonck, J. M. Georges, R. C. Coy, J. C. Bell, and G. W. Roper, "Relationship between mechanical properties and structures of zinc dithiophosphate anti–wear films," Proceedings of the Royal Society of London. Series A: Mathematical, Physical and Engineering Sciences, vol. 455, pp. 4181-4203, December 8, 1999 1999.
[46] M. Aktary, M. T. McDermott, and J. Torkelson, "Morphological evolution of films formed from thermooxidative decomposition of ZDDP," Wear, vol. 247, pp. 172-179, 2001.
[47] D. Uy, S. J. Simko, R. O. Carter Iii, R. K. Jensen, and A. K. Gangopadhyay, "Characterization of anti-wear films formed from fresh and aged engine oils," Wear, vol. 263, pp. 1165-1174, 2007.
[48] P. N. de Aza, C. Santos, A. Pazo, S. de Aza, R. Cuscó, and L. Artús, "Vibrational Properties of Calcium Phosphate Compounds. 1. Raman Spectrum of β-Tricalcium Phosphate," Chemistry of Materials, vol. 9, pp. 912-915, 1997/04/01 1997.

Table 1 Lubricant Composition

Oil Code	Viscosity Grade	Additive concentration – Content (wt %)					Engine lubricant bulk properties				
		P	Zn	Mo	S	FM	Antiwear Type	KV40 (mm^2/s)	KV100 (mm^2/s)	Density (g/cm^3)	Dynamic Viscosity (mPa.s)-ASTMD4684
Oil A - Mid SAPS	SAE 5W-30	0.095	0.102	0	0.22	Yes	ZDDP 11	61.9	10.63	0.854	22120
Oil B - Normal SAPS	SAE 5W-30	0.124	0.140	0	0.5	No	ZDDP 1	56.2	9.84	0.857	18040

Table 2 EDX Spectra of all regions on Polished inserts at 75^{0}C and 105^{0}C with Oil A

Regions	Element (at. %)										Total
	P	Ca	Zn	Fe	S	C	Si	Cr	O	Mn	others	
1	0.7	0.1	0.0	32.4	0.0	58.1	0.1	0.7	7.6	0.3	0.0	100.0
2	0.7	0.1	0.0	32.0	0.0	59.5	0.1	0.6	6.7	0.3	0.0	100.0
3	0.7	0.0	0.1	32.2	0.0	59.2	0.1	0.6	6.7	0.3	0.0	100.0
4	0.1	0.1	0.1	60.3	0.0	38.1	0.3	1.1	0.0	0.0	0.0	100.0
5	2.7	0.1	0.3	41.6	0.4	41.7	0.0	0.8	11.1	1.3	0.1	100.0
6	2.9	0.0	0.0	50.9	0.5	38.1	0.0	0.8	5.2	1.3	0.3	100.0

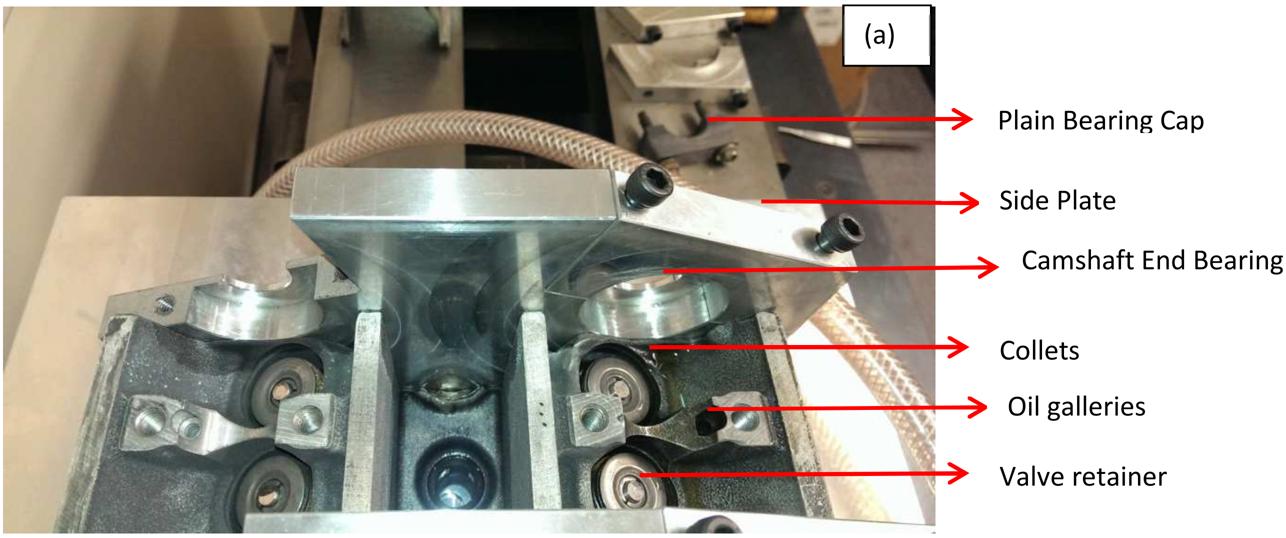

Figure 1a Modified cylinder head (SLICE)

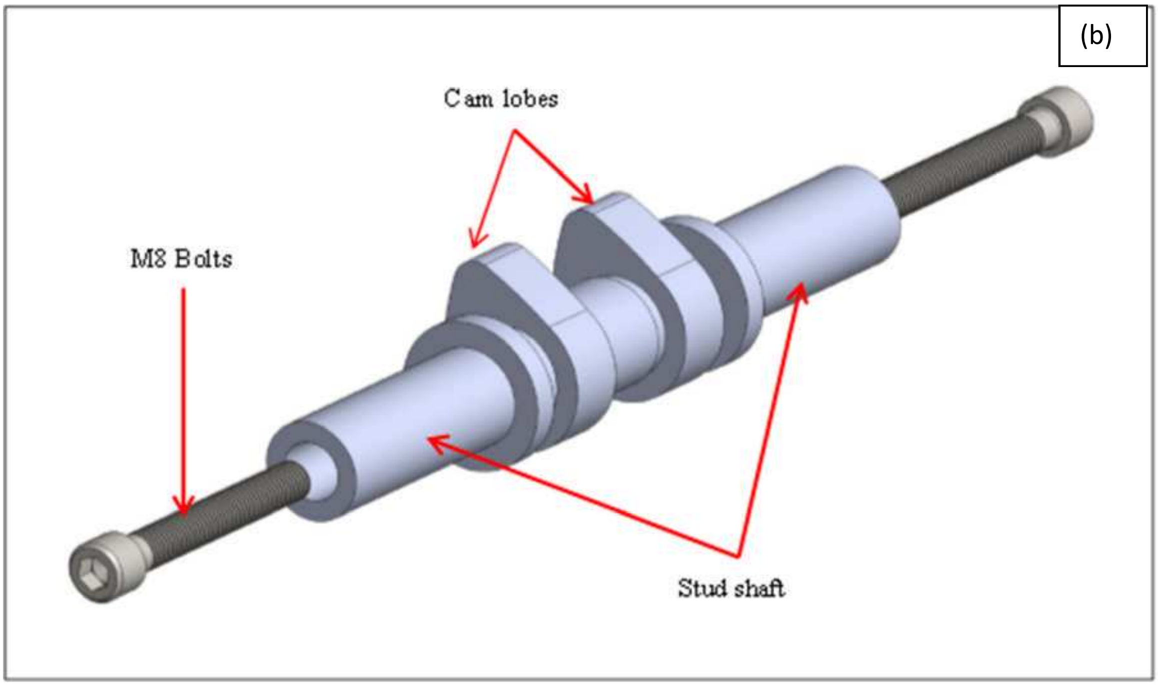

Figure 1b Modified camshaft assembly for single cam rig

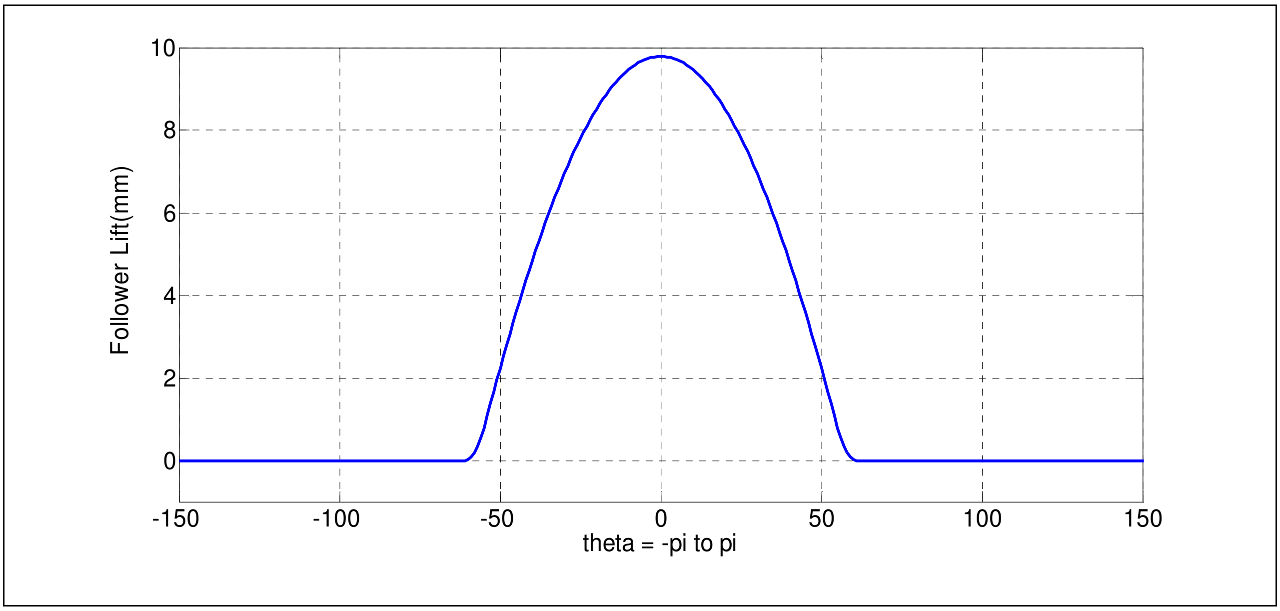

Figure 2 (a) Valve lift

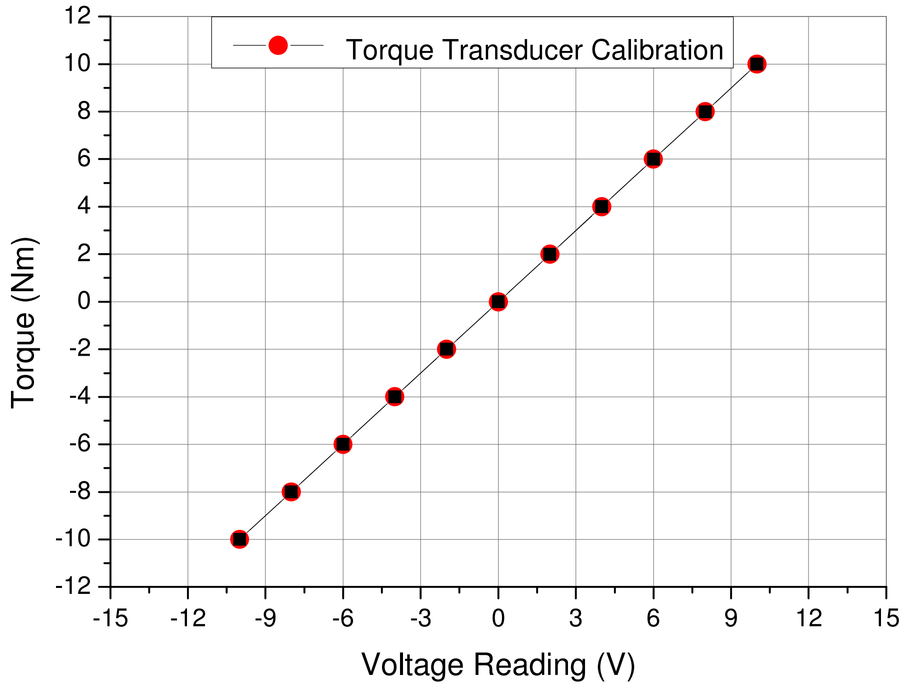

Figure 3 Torque transducer calibration data

Polished inserts with R_a of 0.025µm

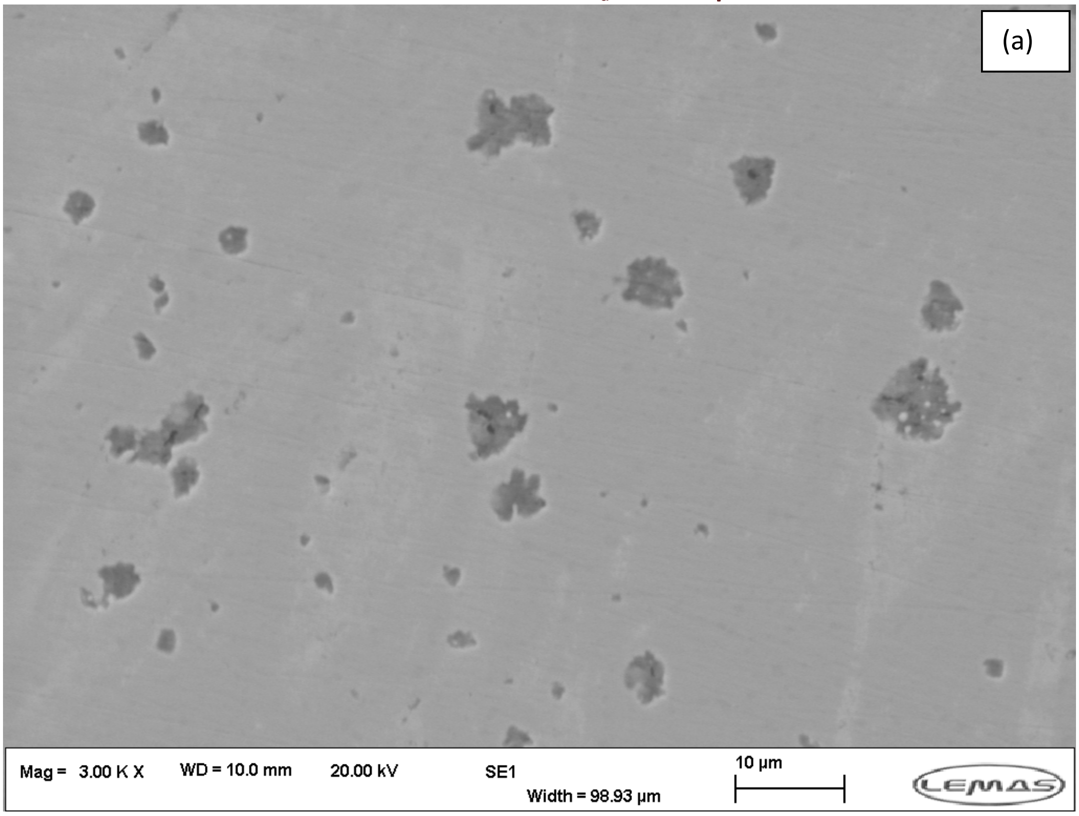

Plain Surface of Polished Inserts

Mn- phosphate inserts with R_a 0.35µm

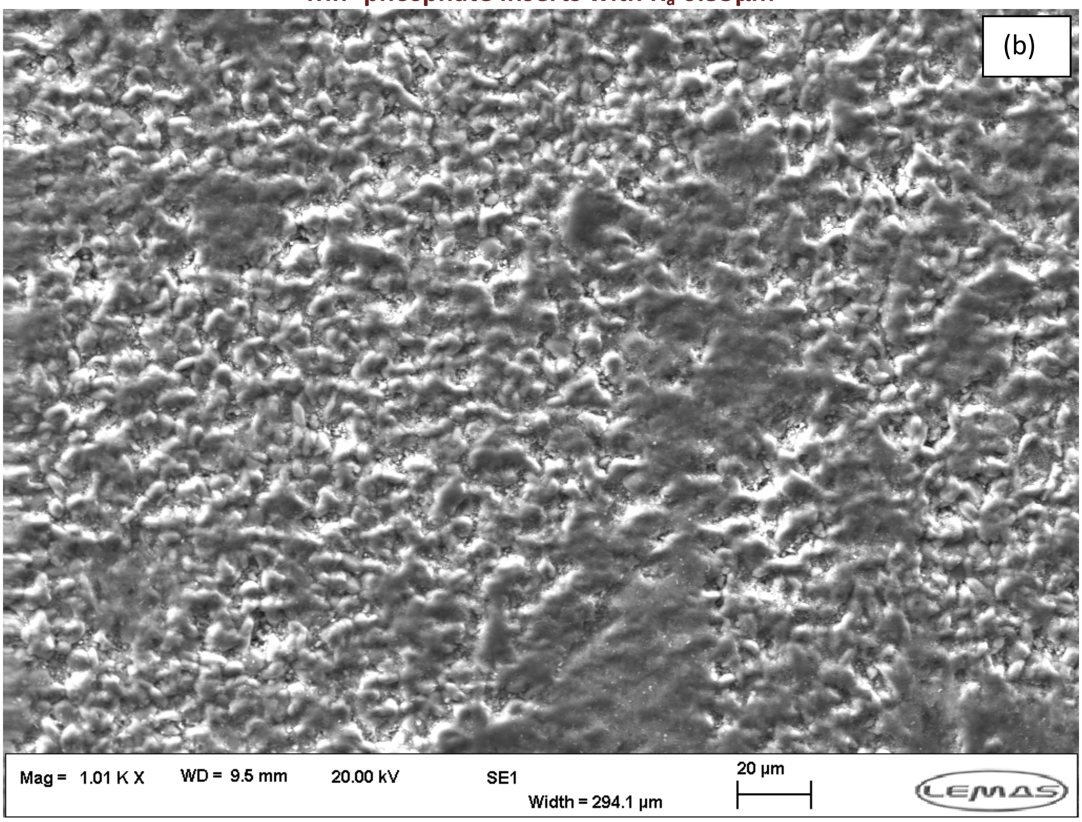

Poly crystalline structure of soft running-in Mn-Phosphate coating

Cast Iron with R_a 0.055µm

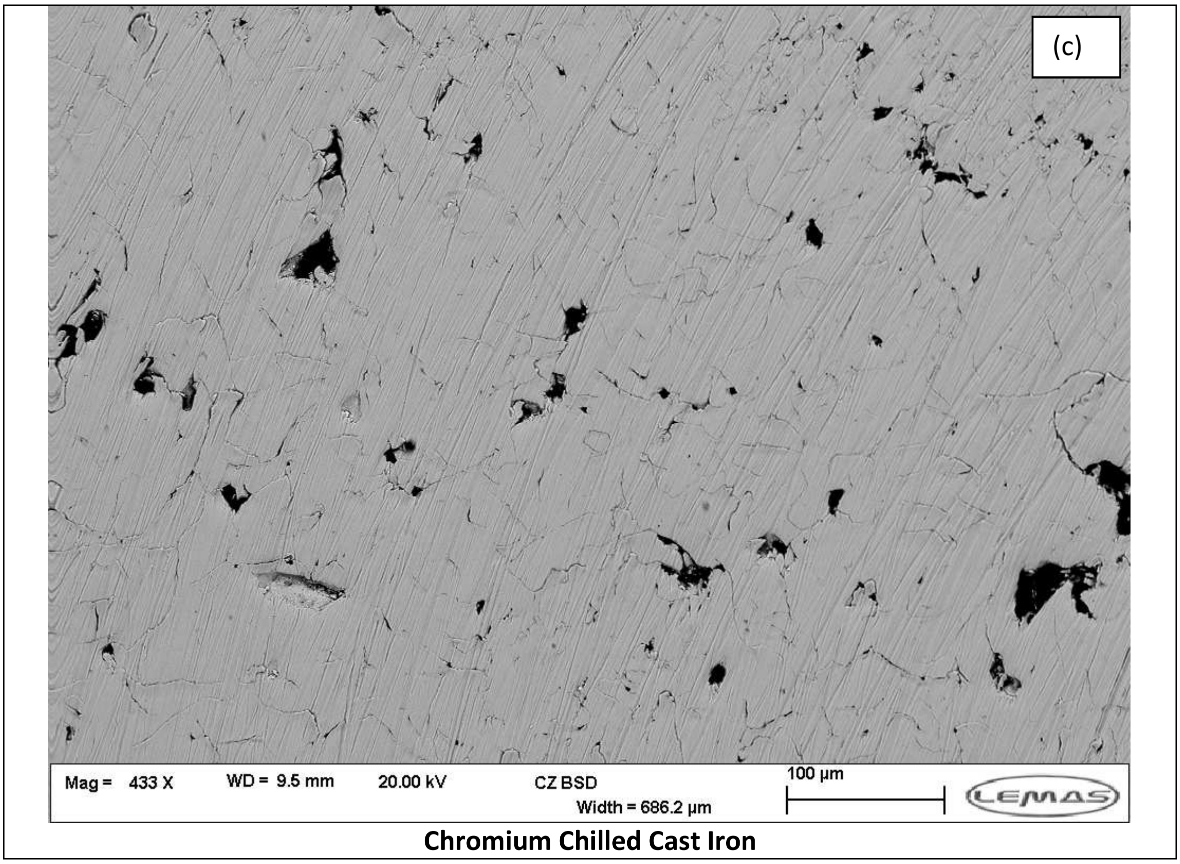

Figure 4 **SEM Image showing (a) Polished surface (b) Polycrystalline structure of Mn-phosphate (c) Chromium chilled cast Iron**

Figure 4d **Bucket and Inserts**

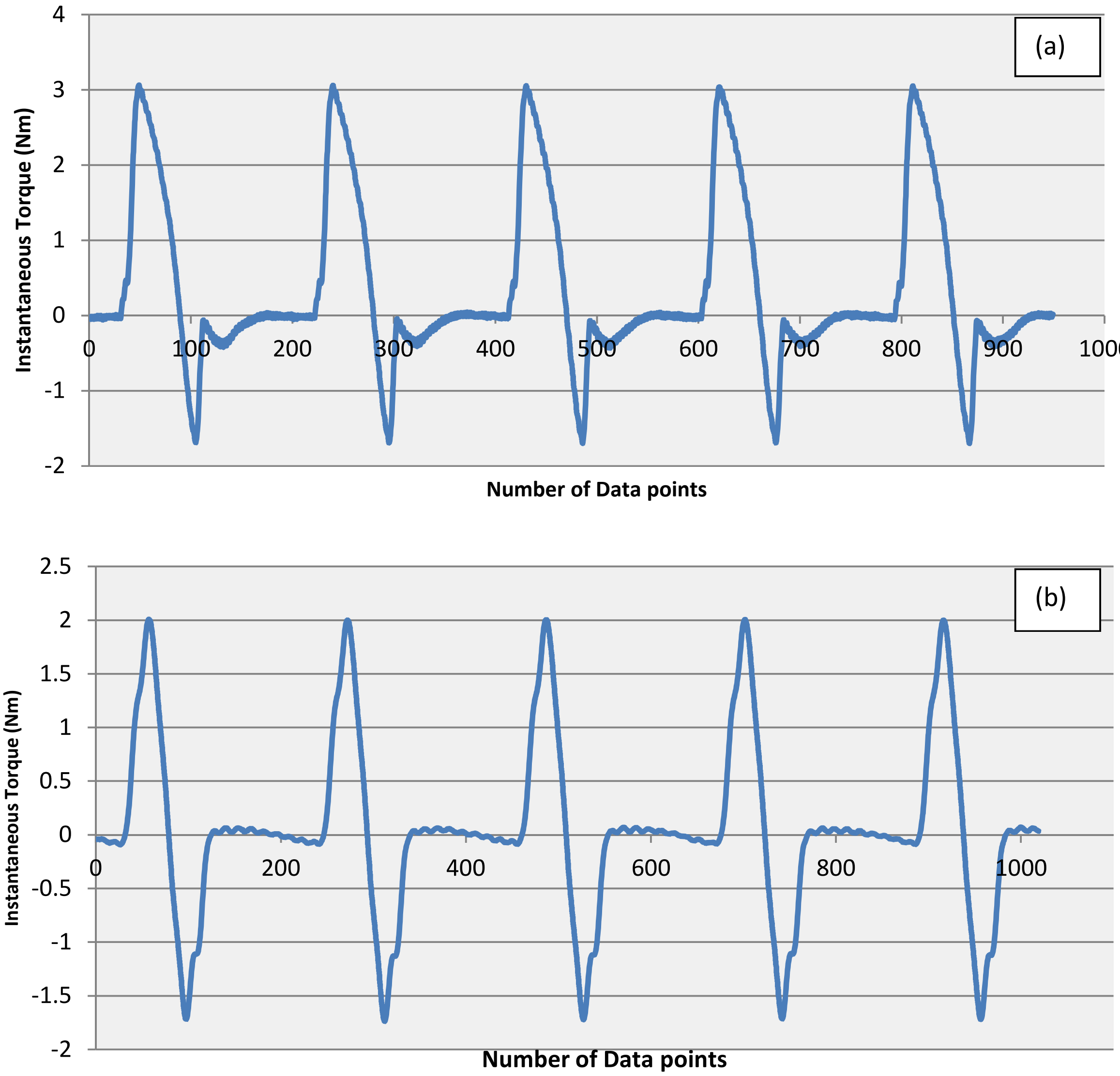

Figure 5 **Torque transducer output voltages at camshaft speed of (a) 300 rpm and (b) 2100 rpm**

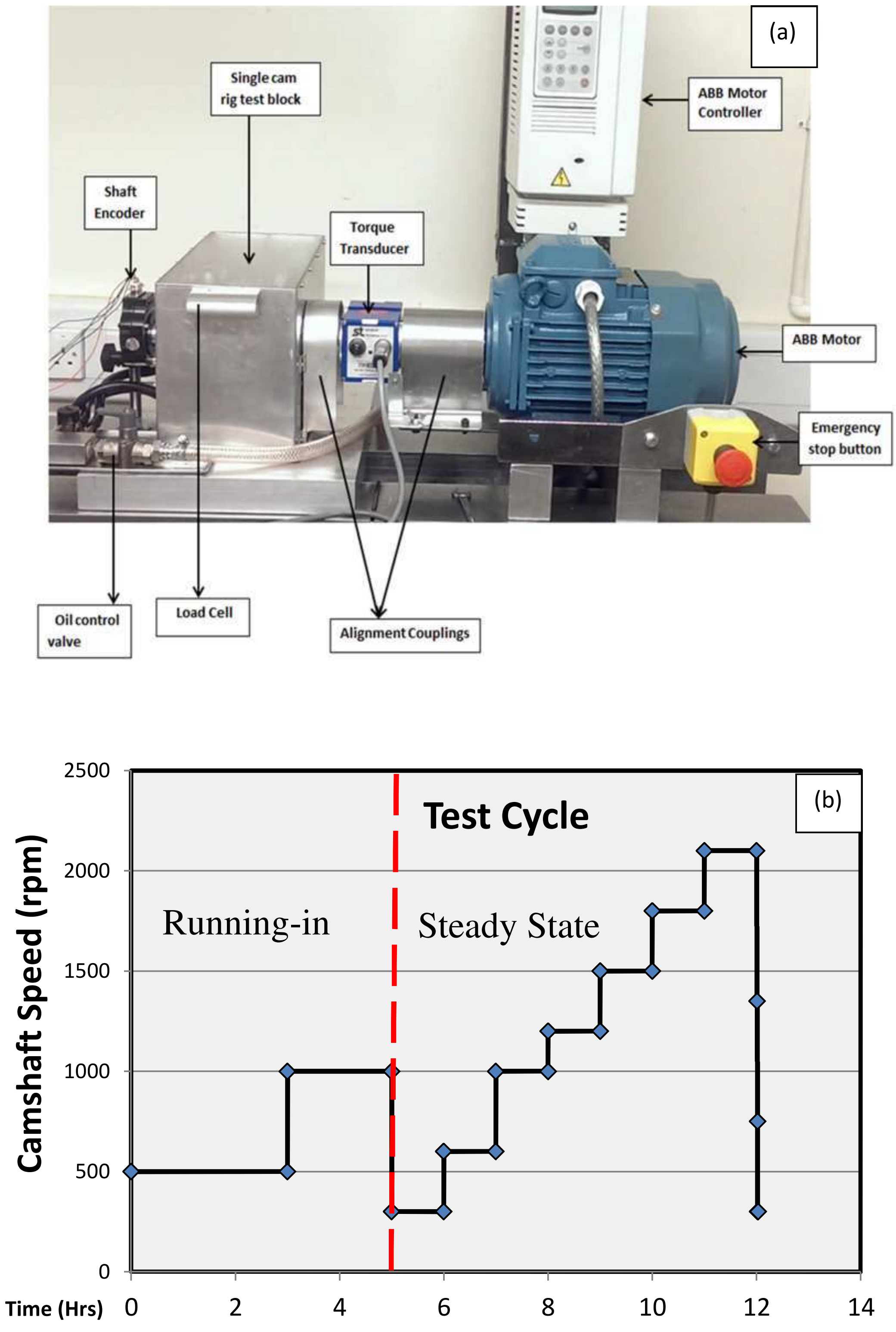

Figure 6 (a) Schematic of newly developed single cam follower rig (b). Camshaft test cycle

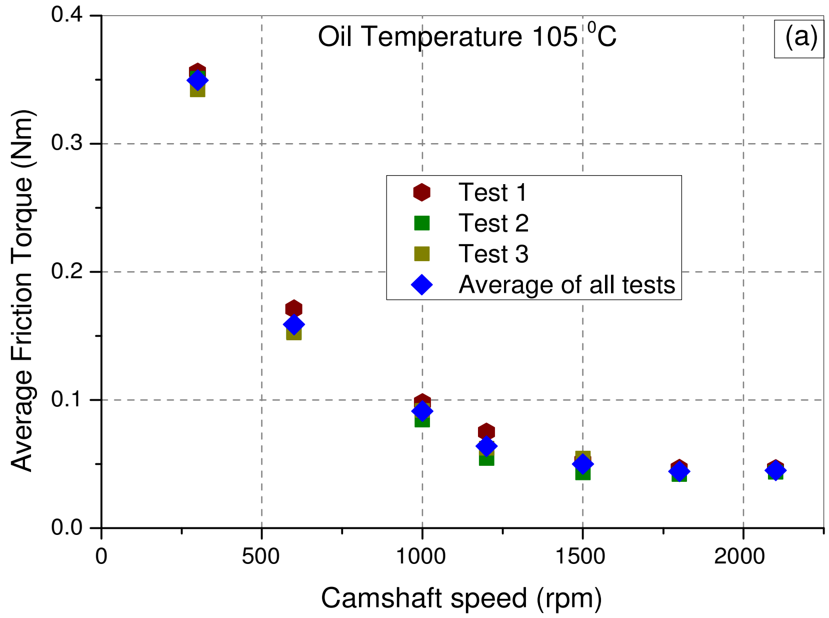

Figure 7a **Friction torque data on newly developed single cam rig showing good repeatability with oil A against polished inserts at 105^{0}C**

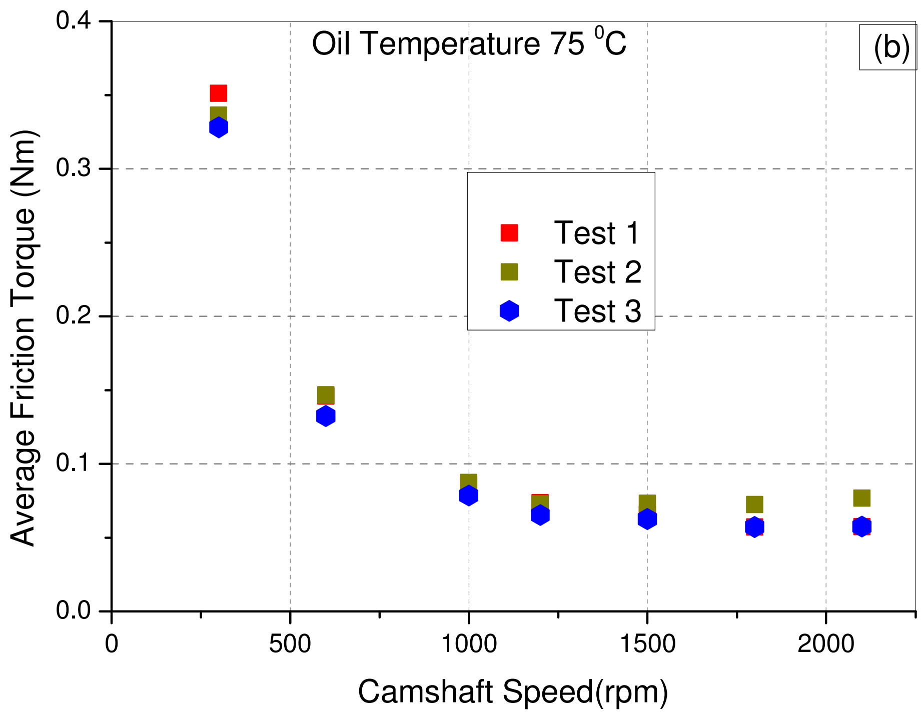

Figure 7b **Friction torque data on newly developed single cam rig showing good repeatability with oil A against Mn-phosphate inserts at 75^{0}C**

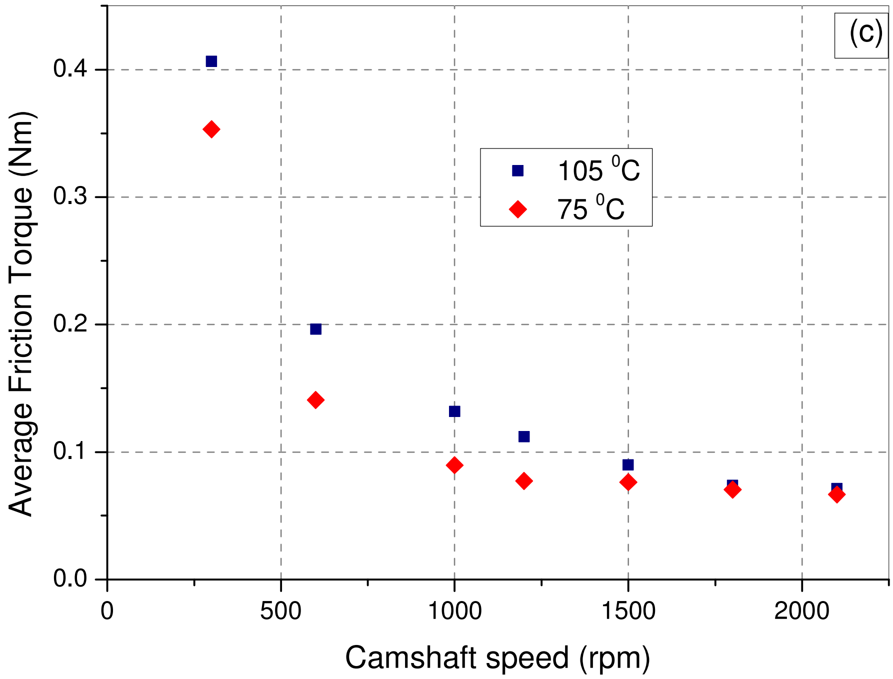

Figure 7c **Effects of temperature on newly developed single cam test rig with Mn-phosphate coating.**

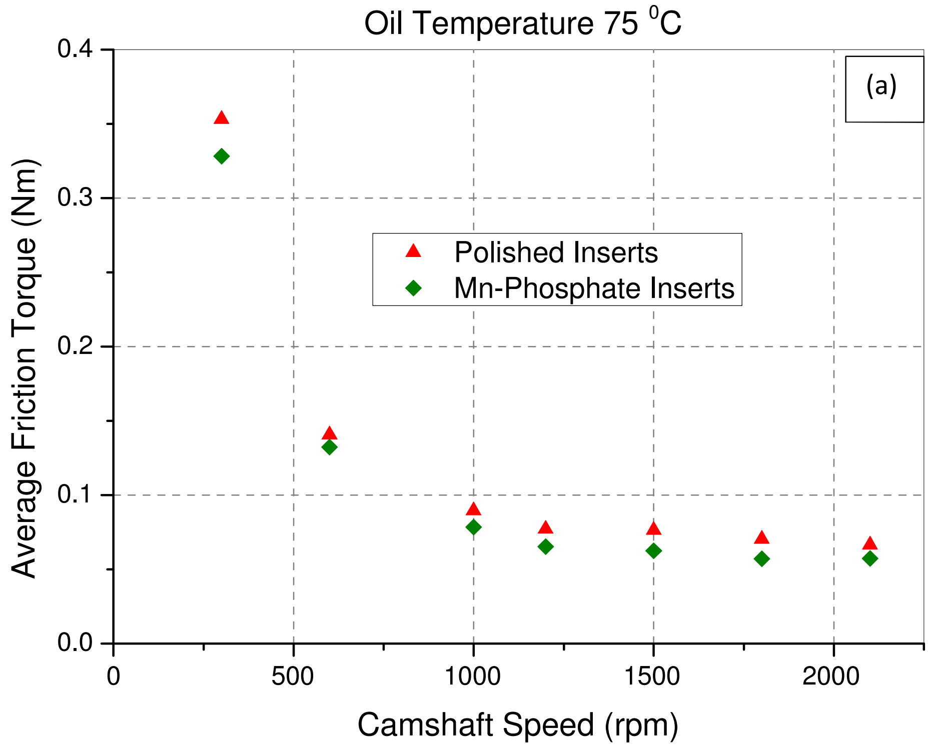

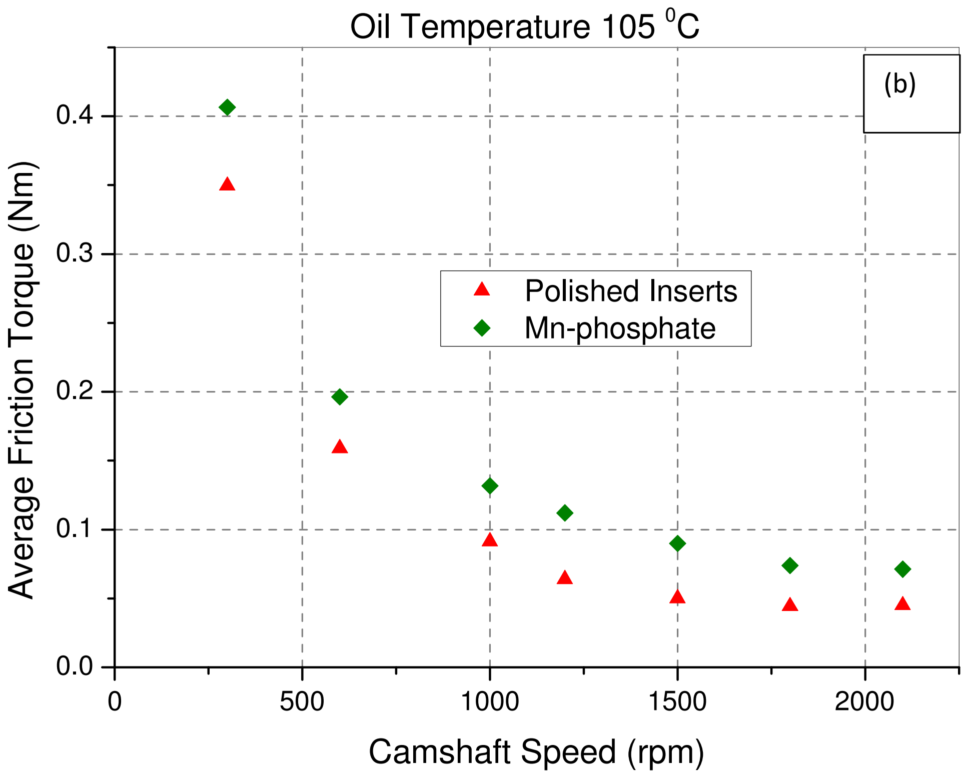

Figure 8 **Effect of surface finishing on friction torque with the newly developed single cam rig with (a) Oil A at 75^{0}C (b) Oil A at 105^{0}C**

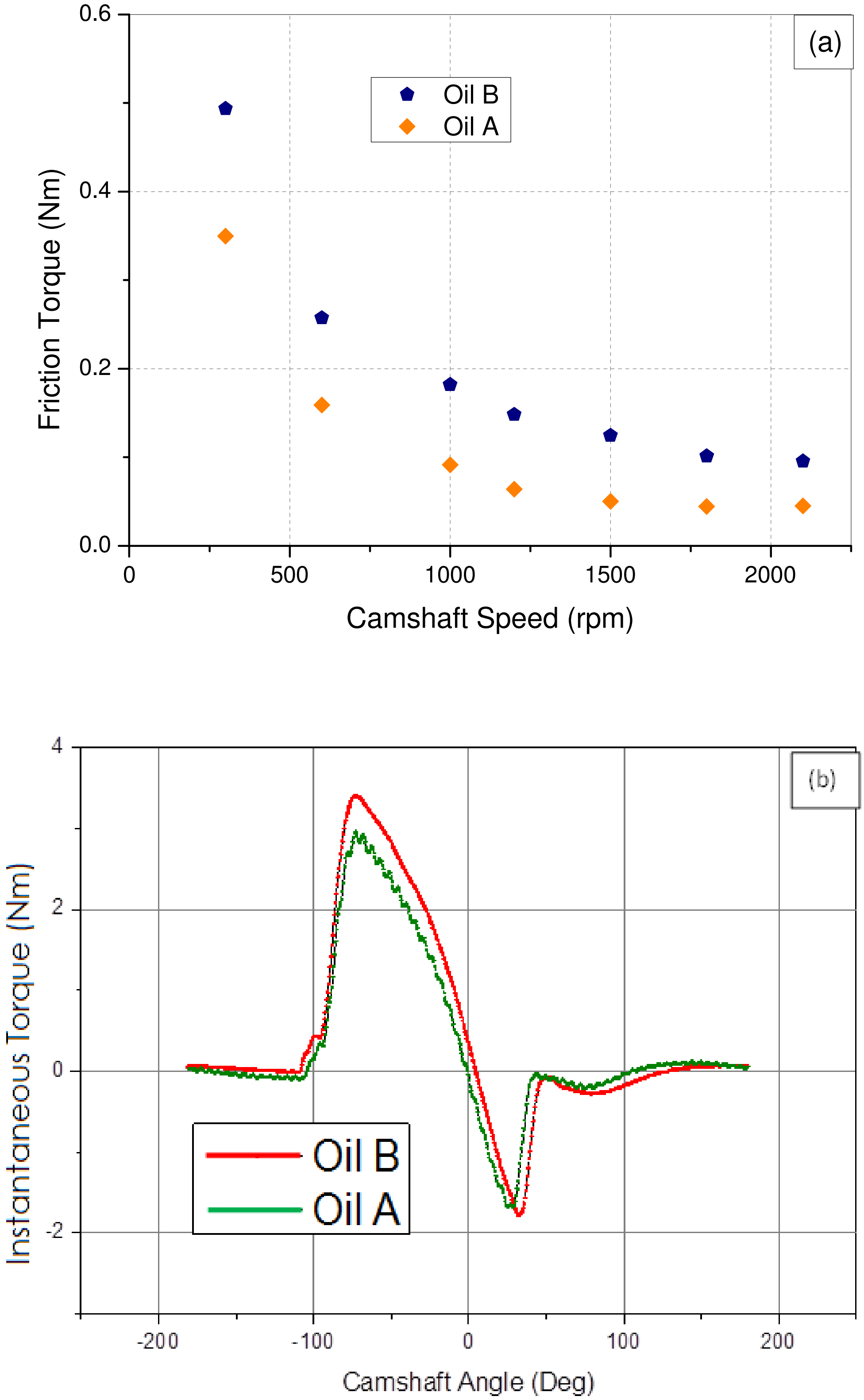

Figure 9 **Effect of oil type on friction torque (a) Polished inserts at 105 ^{0}C (b) Instantaneous torque across cam profile at 300 rpm with polished Inserts at 105 ^{0}C**

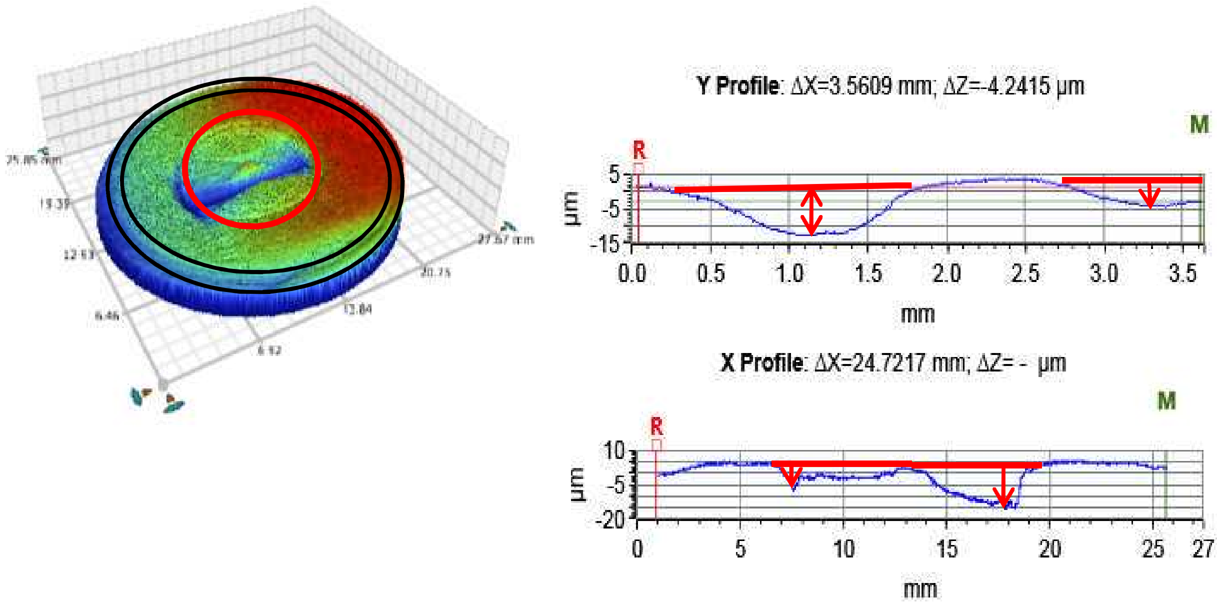

Figure 10 Wear scar measurement procedure from Inserts

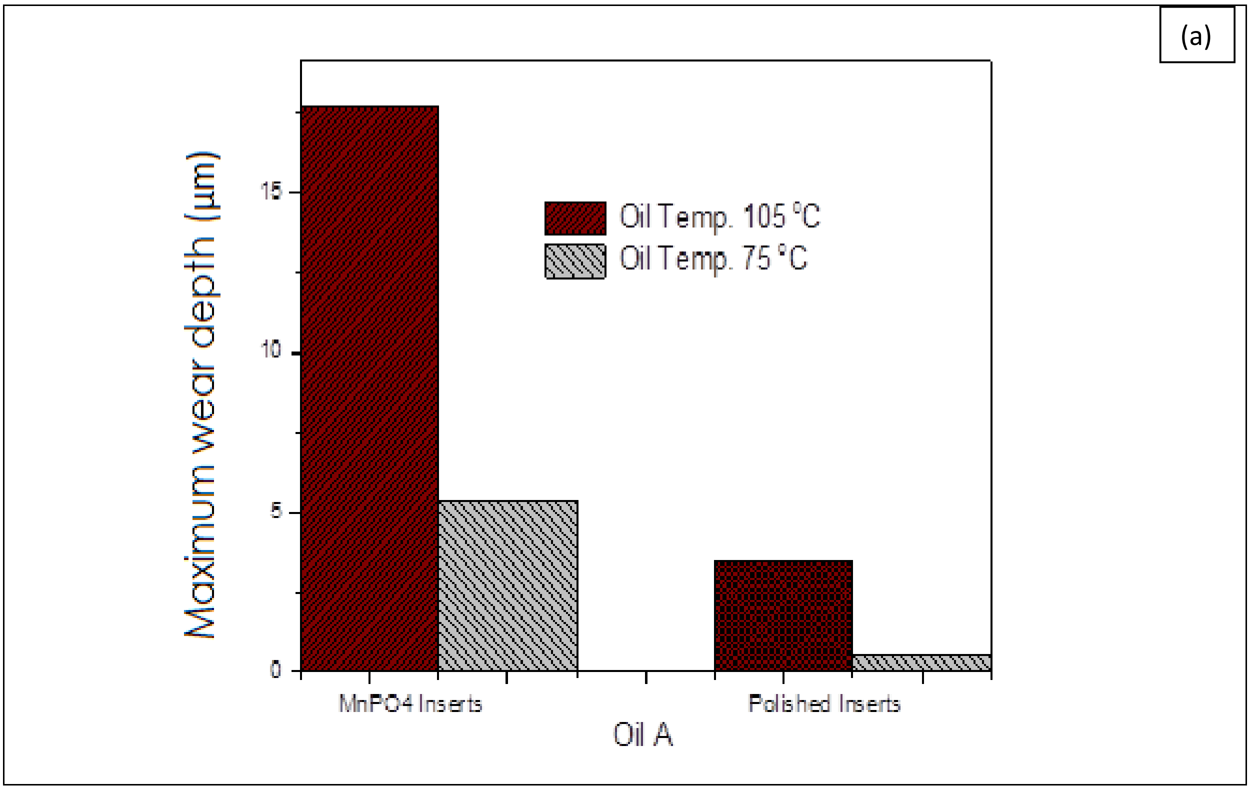

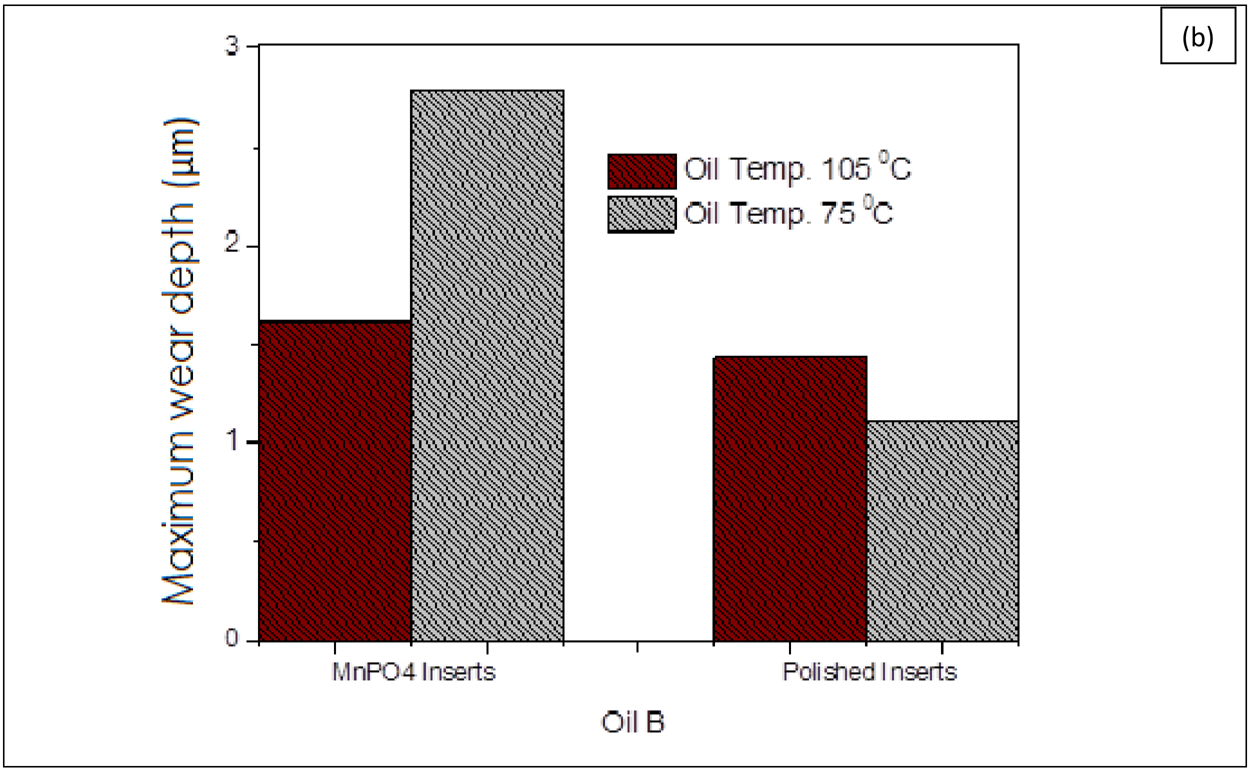

Figure 11 **Maximum Wear Depths with (a) Mid SAPS Oil A and (b) Normal SAPS Oil B**

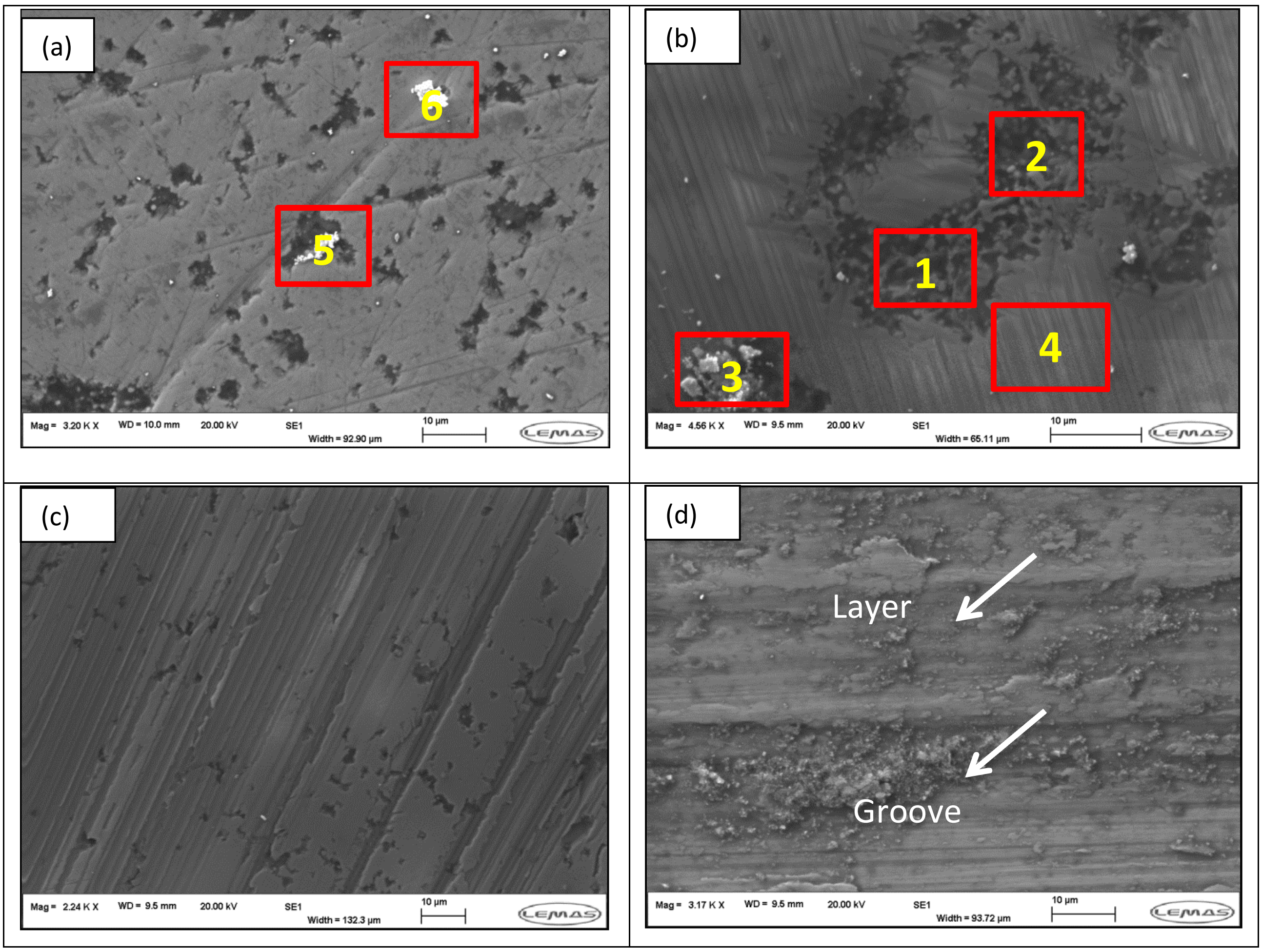

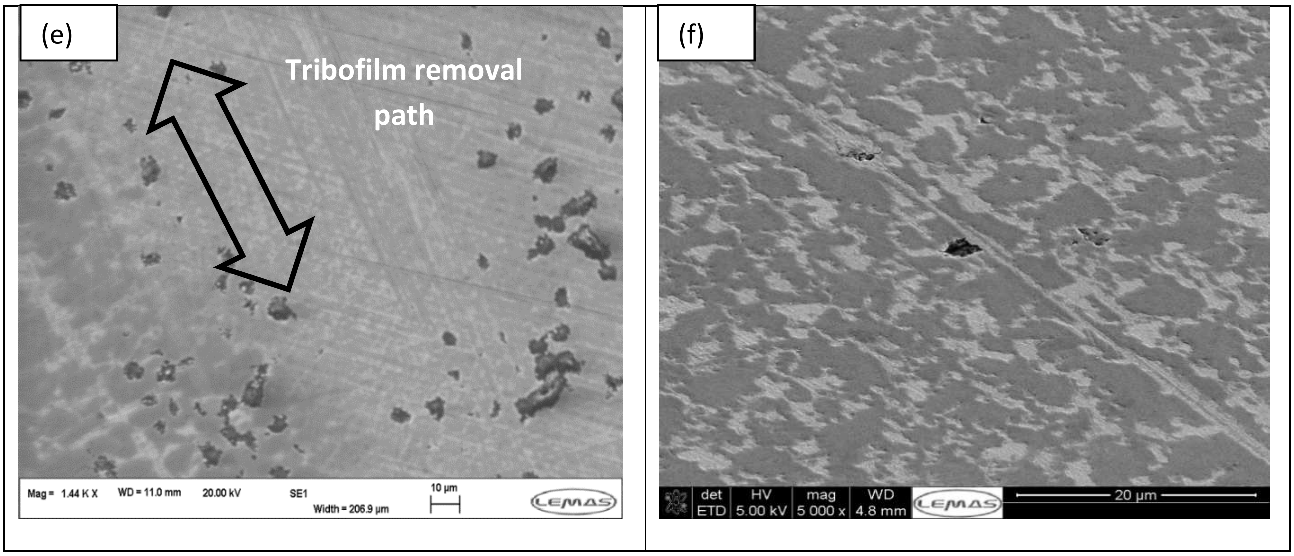

Figure 12 Scanning Electron Micrograph (a) Oil A with Polished inserts at 75 ^{0}C – Top left (b) Oil A with Polished inserts at 105 ^{0}C – Top Right (c) Oil A with Mn-phosphate at 75 ^{0}C – Mid left (d) Oil A Mn-phosphate at 105^{0} – Mid Right (e) Polished inserts against Oil B at 75 ^{0}C – Bottom left (f) Polished inserts against oil B at 105 ^{0}C – Bottom Right

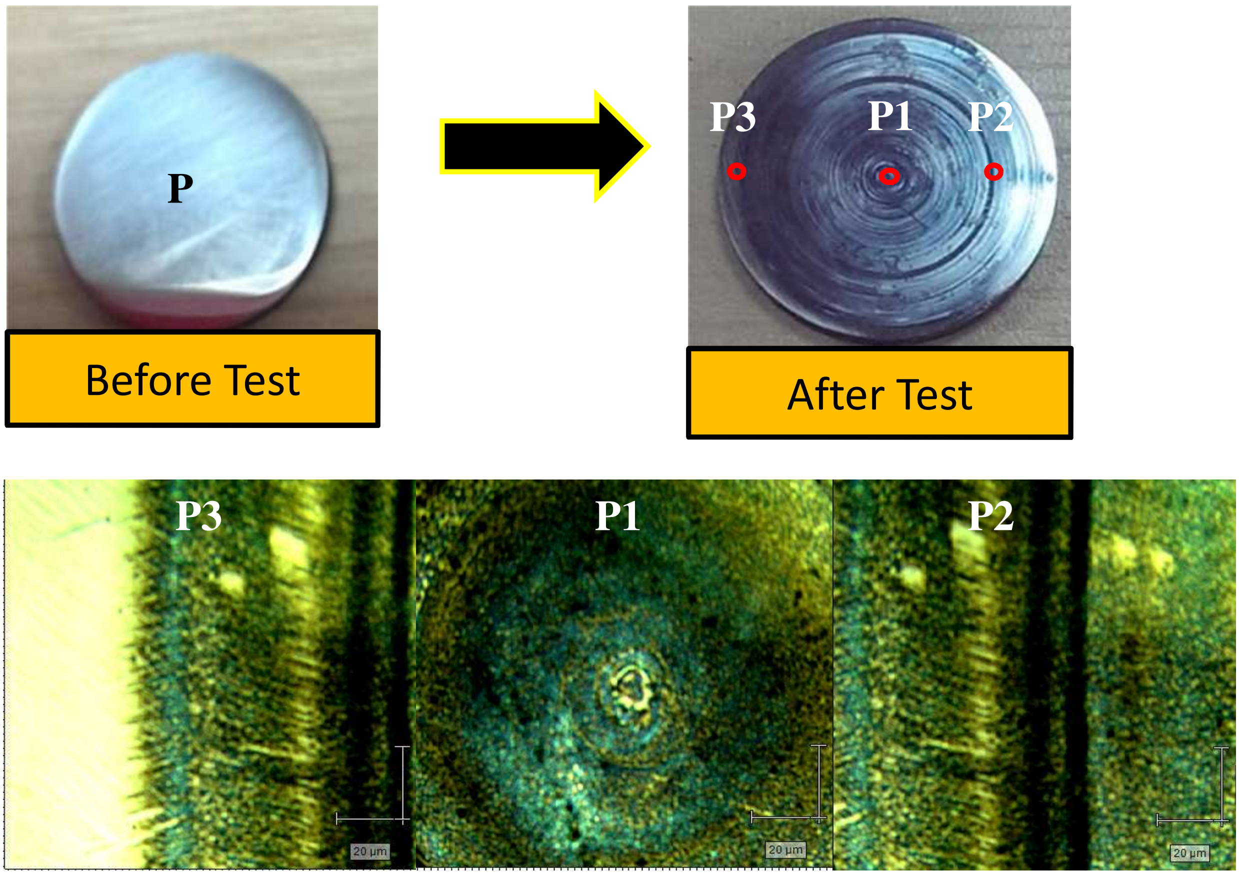

Figure 13 Raman Image (a) Polished insert wear scar – P1 (b) Polished insert Wear scar - P2 (c) Polished insert wear scar – P3

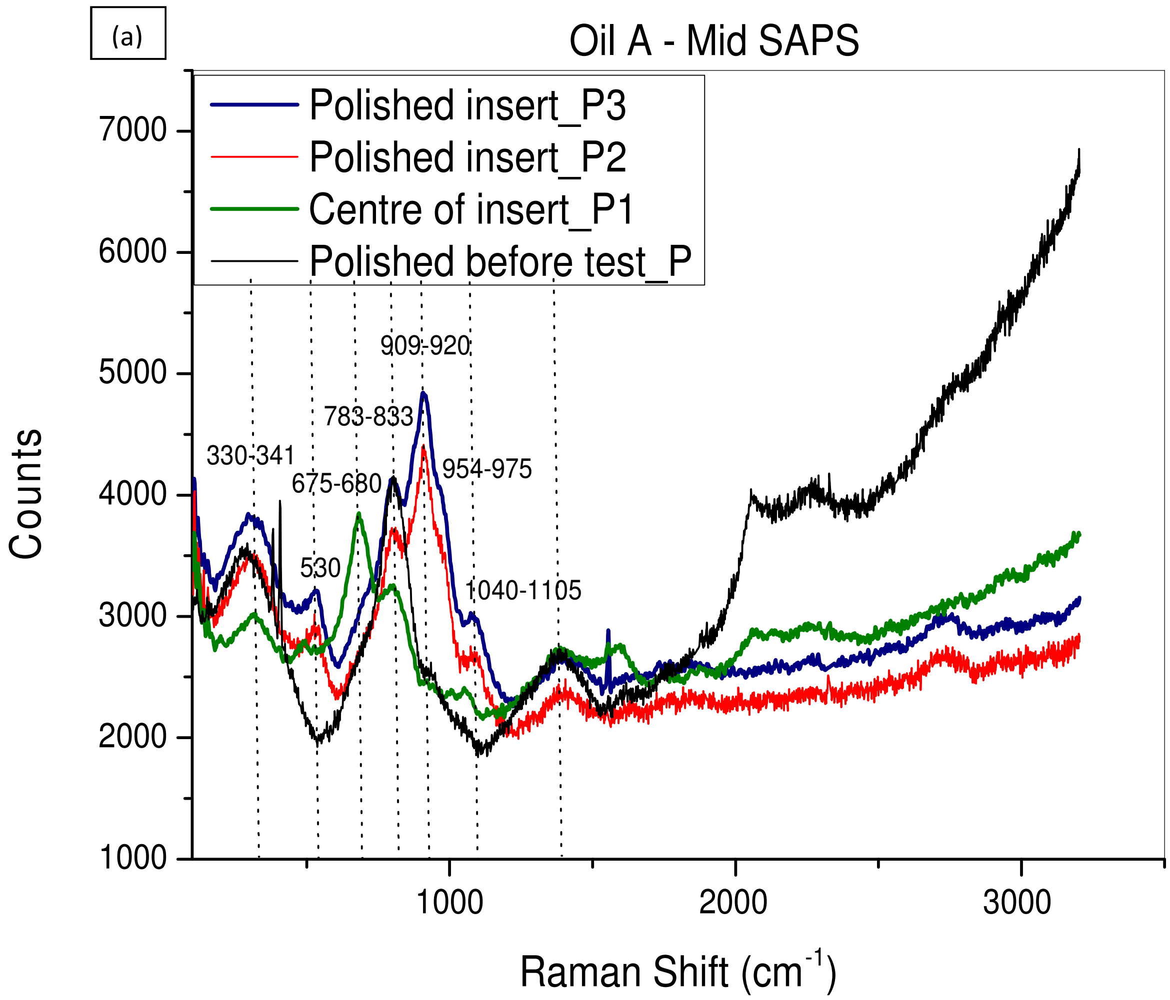
(a)
Oil A - Mid SAPS
Polished insert_P3
Polished insert_P2
Centre of insert_P1
Polished before test_P
909-920
783-833
330-341
675-680
954-975
530
1040-1105
Counts
7000
6000
5000
4000
3000
2000
1000
1000
2000
3000
Raman Shift (cm-1)

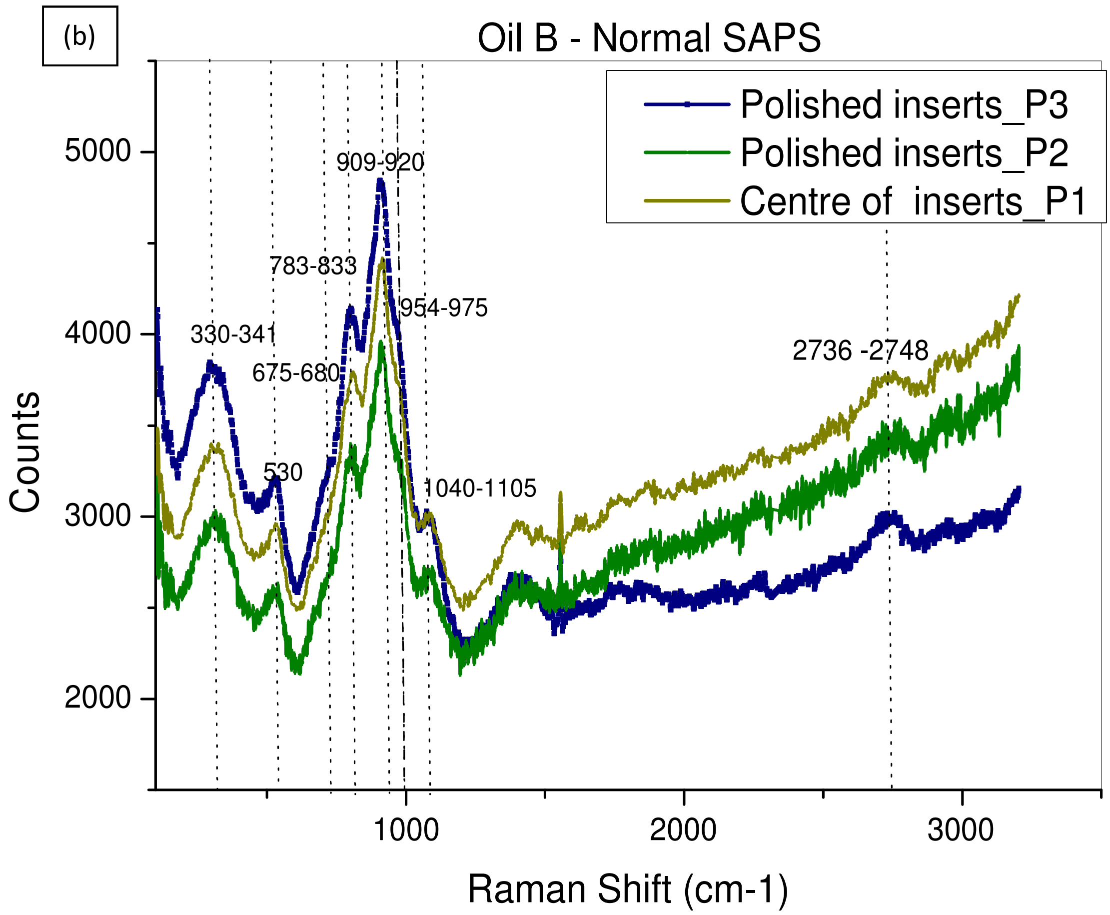

Figure 14 Raman Spectra of films formed on Polished Inserts at P1, P2, and P3 at 105 ^{0}C by (a) Oil A – Mid SAPS and (b) Oil B – Normal SAPS

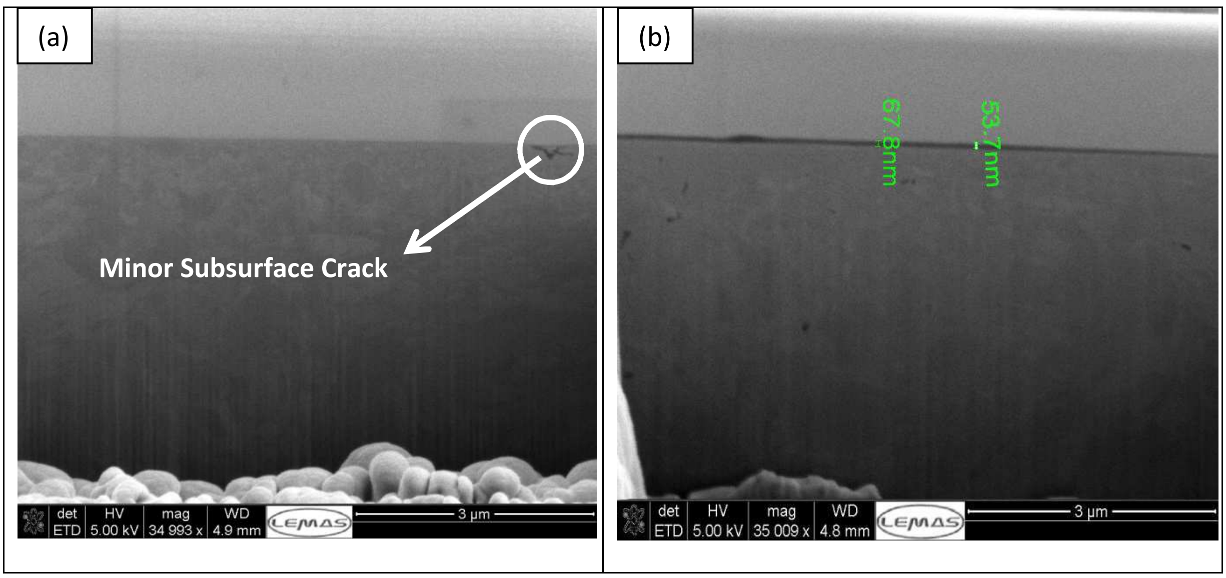

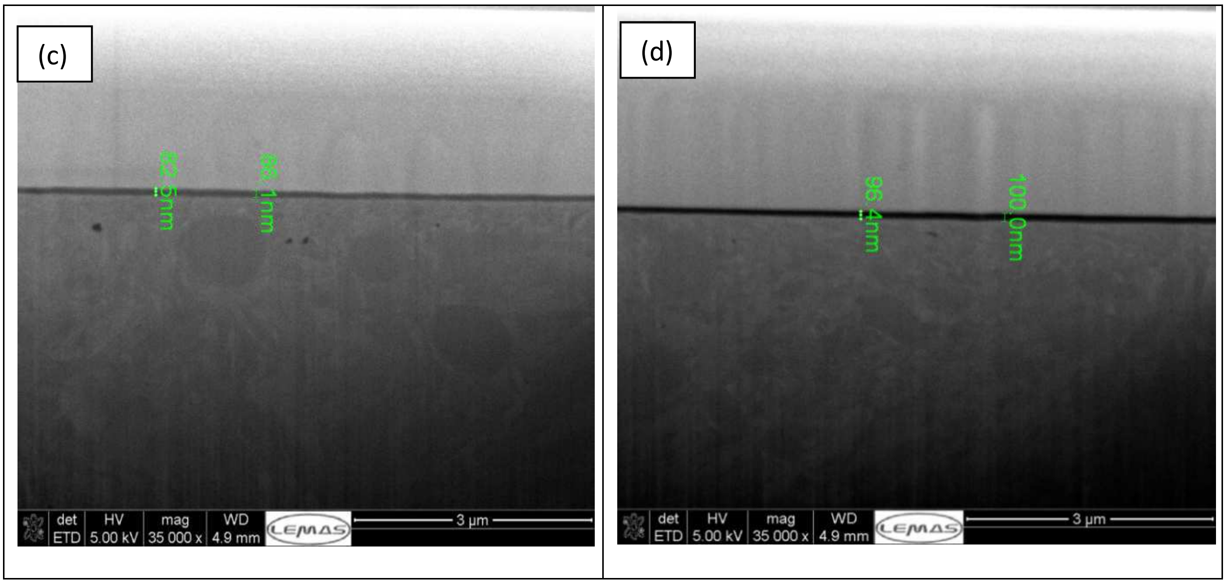

Figure 15 FIB-SEM showing tribofilm thickness with (a) Oil FFA at P1- top left (b) On track P2 – top right (c) Oil B at P1 –bottom left (d) Oil B at P2 – Bottom right